

# Sample and Expand: Discovering Low-rank Submatrices With Quality Guarantees

Martino Ciaperoni<sup>1\*</sup> (✉), Aristides Gionis<sup>2</sup>, and Heikki Mannila<sup>3</sup>

<sup>1</sup> Scuola Normale Superiore, Italy

[martino.ciaperoni@sns.it](mailto:martino.ciaperoni@sns.it)

<sup>2</sup> KTH Royal Institute of Technology, Sweden

[argioni@kth.se](mailto:argioni@kth.se)

<sup>3</sup> Aalto University, Finland

[heikki.mannila@aalto.fi](mailto:heikki.mannila@aalto.fi)

**Abstract.** The problem of approximating a matrix by a low-rank one has been extensively studied. This problem assumes, however, that the whole matrix has a low-rank structure. This assumption is often false for real-world matrices. We consider the problem of discovering submatrices from the given matrix with bounded deviations from their low-rank approximations. We introduce an effective two-phase method for this task: first, we use sampling to discover small nearly low-rank submatrices, and then they are expanded while preserving proximity to a low-rank approximation. An extensive experimental evaluation confirms that the method we introduce compares favorably to existing approaches.

**Keywords:** Low-rank approximation · submatrix detection.

## 1 Introduction

Low-rank approximation has emerged as a fundamental task in many data-analysis applications, including machine-learning pipelines [32], large language models [17], recommender systems [20], image compression and denoising [15]. The goal of low-rank approximation is to represent an input matrix as accurately as possible using a small number of row and column vectors.

For decades, the *singular value decomposition* (SVD), with the closely related principal component analysis (PCA), has remained the gold standard for low-rank approximation [14]. Despite its success, SVD has certain limitations. Among others, when applying SVD we aim to find a low-rank approximation for the entire input matrix. This assumption can be rather restrictive, as in real-world data it might be that only certain submatrices are well approximated by low-rank structures. For instance, in ratings data originating in movie recommender systems, low-rank submatrices occur because subsets of users may share a similar taste only for a subset of movies. Similar local patterns could be observed in data coming from other domains, such as market-basket analysis, image processing, and biology [7]. The SVD can fail to identify local low-rank submatrices.

---

\* The work was done while the author was at Aalto University.

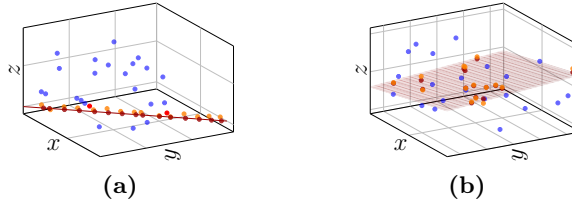


Fig. 1: Example. A subset of data points (in orange) in the 3-dimensional space are close to their projection (in red) onto a line in the  $xy$ -plane (a) or to a plane in the 3-dimensional space (b), while other points (in blue) can be further away.

**Existing approaches to find local low-rank submatrices.** The task of identifying submatrices that are well described by low-rank structures has been largely overlooked until recently [7]. Existing work in this direction is based primarily on the SVD, and does not provide any guarantee on the quality of the approximation for the identified submatrices.

**Our approach.** In this work, we adopt a different perspective on discovering local low-rank patterns, and we address the problem of identifying submatrices that are guaranteed to be close to a low-rank approximation. Our quality guarantees hold with respect to an approximation that can be easily interpreted in terms of the original data, which can be particularly valuable for applications in different domains. For example, near-rank-1 submatrices can be accurately approximated by each row in the submatrix being colinear with a single row. Unlike previous work, our work does not directly rely on the SVD. Nearly-low-rank submatrices correspond to subsets of points (matrix rows) that approximately lie on a low-dimensional subspace, for a subset of dimensions (matrix columns). For rank equal to 1, which is a particularly interesting case, the points approximately lie on a line through the origin, and for rank equal to 2 the points are close to a plane through the origin, as in the example of Figure 1, which shows data points identifying a  $15 \times 2$  near-rank-1 submatrix and a  $15 \times 3$  near-rank-2 submatrix.

While SVD may fail to reveal dense lines in the data, it is possible to find such structures by sampling. A naïve approach would be to sample subsets of points and dimensions until a large set of nearly-collinear points is found. However, this procedure quickly becomes inefficient. Instead, to identify points approximately distributed along a line, we introduce a method that only relies on sampling in an initialization phase to find a minimal structure that can exhibit this property, i.e., two points in two-dimensions. In a subsequent phase, the  $2 \times 2$  submatrix is expanded deterministically to obtain the entire subset of points and dimensions associated with the target line. Based on such a two-phase method, we discover arbitrary submatrices that admit low-rank approximations that can be easily interpreted in terms of the original submatrix rows or columns, and are supported by quality guarantees. A real-world example is given in Figure 2.

**Our contributions.** Our main contributions can be summarized as follows.

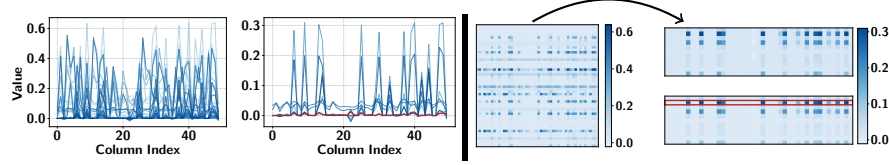


Fig. 2: HYERSPECTRAL dataset. On the left, we show the values of the rows in a  $50 \times 50$  matrix and the nearly-proportional values of the rows in a near-rank-1  $11 \times 44$  submatrix discovered by our method. On the right we show the matrix and, next to it, the discovered submatrix (top) and its accurate approximation expressing each row as collinear with the row highlighted in red (bottom).

- We formalize the problem of finding submatrices that are provably close to a low-rank approximation.
- We introduce an effective method for finding submatrices that are provably close to rank 1. Then, we generalize this method to the case of rank- $k$  submatrices.
- We analyze the theoretical properties of the method we introduce.
- We demonstrate the advantages of our method over previous work.

**Roadmap.** The rest of the paper is organized as follows. In Section 2 we discuss related work. Section 3 introduces the notation used throughout the paper as well as key preliminary concepts. In Section 4 we present the problem we study and in Section 5 we illustrate our method to address it. In Section 6 we analyze the properties of the method, and in Section 7 we assess its empirical performance. Finally, Section 8 provides conclusions.

## 2 Related Work

**Low-rank matrix approximation.** Low-rank approximation techniques are widely used to decompose a matrix into simpler components, capturing essential patterns while reducing noise and dimensionality. The SVD and the related PCA are among the most popular techniques [14]. Nonnegative matrix factorization techniques [12] have become popular in applications where the goal is to decompose data in nonnegative components. Boolean matrix decomposition relies on boolean algebra instead of linear algebra [25]. Column subset selection [4] and the CUR decomposition [23] have emerged as more interpretable alternatives to the SVD. In 2019, Gillis and Shitov [13] studied the problem of low-rank approximation to minimize the maximum entry-wise deviation. More recently, an approach to low-rank approximation that accounts for multiplicative effects was introduced [6].

**Local low-rank matrix approximation.** Relatively less research has been conducted for finding decompositions that do not assume a *global* low-rank structure, which is the focus of our paper. The goal here is to find submatrices that are *locally* well-approximated by a low-rank structure. A simple heuristic to local

low-rank approximation is obtained by imposing a sparsity constraint on matrix decomposition, and sparse PCA [24] is a prominent example of such methods.

Doan and Vavasis proposed the problem of recovering near-rank-1 submatrices by framing it as a convex-optimization problem [10]. Lee et al. [20] introduced the LLORMA method to address matrix-completion tasks while relaxing the assumption that the entire matrix has low rank. LLORMA approximates the entire input matrix, and thus, it is fundamentally different from our work, which focuses on detecting local low-rank patterns. On the other hand, the problem we study finds application in matrix completion, as shown by the work of Ruchansky et al. [26], which introduces the SVP method to quickly detect low-rank submatrices with the ultimate goal of improving the accuracy in matrix completion. While SVP cannot discover arbitrary low-rank submatrices, Dang et al. [7] introduced the RPSP method, which addresses this lack of generality. The core idea behind RPSP is to sample submatrices and count the number of times that each entry belongs to a low-rank submatrix. Like RPSP, our method targets arbitrary near-low-rank submatrices. Unlike previous methods, our method can in principle identify submatrices that are close to a specific target rank.

**Co-clustering, projective clustering, and subspace clustering.** Co-clustering algorithms [9] simultaneously cluster the rows and columns of a matrix. Although co-clustering algorithms can be used for detecting low-rank submatrices, they cannot generally discover such structures, except in specific cases where the values of the low-rank submatrices deviate significantly from the background. Projective clustering and subspace clustering are also related problems. In projective clustering [1], the goal is to partition the data into subsets such that the points in each subset are close to each other in some subspace. In subspace clustering [31] the goal is to find a representation of the input data as a union of different subspaces. In general, clustering problems are fundamentally different from the problem we study, as they seek a partitioning of the entire data matrix.

### 3 Preliminaries

**Notation and basic definitions.** Matrices are denoted by upper-case boldface letters, and we use  $\mathbf{D}$  to denote the input data matrix.  $\mathbf{D}_{i,j}$  indicates the entry of  $\mathbf{D}$  in row  $i$  and column  $j$ , while the  $i$ -th row and  $j$ -th column of  $\mathbf{D}$  are denoted by  $\mathbf{D}_{i,:}$  and  $\mathbf{D}_{:,j}$ , respectively. Sets are denoted by upper-case letters and scalars by lower-case letters. Vectors are denoted by lower-case boldface letters, e.g.,  $\mathbf{x} = (x_1, \dots, x_d)$ . We denote the  $L_2$  (or Euclidean) norm of a vector  $\mathbf{x}$  as  $\|\mathbf{x}\|_2$  and the inner product between two vectors  $\mathbf{x}$  and  $\mathbf{y}$  as  $\mathbf{x}^T \mathbf{y}$ . We consider different matrix norms: the Frobenius norm  $\|\mathbf{D}\|_F = (\sum_{i,j} |\mathbf{D}_{i,j}|^2)^{1/2}$ , the spectral norm  $\|\mathbf{D}\|_2 = \sup_{\|\mathbf{x}\|_2 \leq 1} \|\mathbf{D}\mathbf{x}\|_2$ , and the max norm  $\|\mathbf{D}\|_{\max} = \max_{i,j} |\mathbf{D}_{i,j}|$ . We use  $\|\mathbf{D}\|_*$  with  $* = \{2, F, \max\}$  to indicate the above norms. We refer to the total number of entries of a (sub)matrix  $\mathbf{D}$  as its *size*, which is also simply denoted by  $|\mathbf{D}|$ , if there is no risk of confusion with the entry-wise absolute value. For a matrix  $\mathbf{X}$ , we denote by  $\hat{\mathbf{X}}$  a low-rank approximation of  $\mathbf{X}$  and by  $\mathbf{E}_{\mathbf{X}, \hat{\mathbf{X}}}$  the difference  $\mathbf{E}_{\mathbf{X}, \hat{\mathbf{X}}} = \mathbf{X} - \hat{\mathbf{X}}$ .

**Orthogonal projections.** Given a nonzero vector  $\mathbf{x}$  and a vector  $\mathbf{y}$ , the *orthogonal projection* of  $\mathbf{y}$  onto  $\mathbf{x}$  is given by  $\text{Proj}_{\mathbf{x}} \mathbf{y} = (\mathbf{y}^T \mathbf{x}) / (\mathbf{x}^T \mathbf{x}) \mathbf{x}$ . Similarly, given a matrix  $\mathbf{B}$  and a matrix  $\mathbf{A}$  with linearly independent columns, the *orthogonal projection* of  $\mathbf{B}$  onto the column space of  $\mathbf{A}$  is given by  $\text{Proj}_{\mathbf{A}} \mathbf{B} = \mathbf{A} \mathbf{A}^+ \mathbf{B}$ , where  $\mathbf{A}^+ = (\mathbf{A}^T \mathbf{A})^{-1} \mathbf{A}^T$  is the *Moore-Penrose pseudoinverse* of  $\mathbf{A}$ . The orthogonal projection  $\text{Proj}_{\mathbf{A}} \mathbf{B}$  is the closest matrix to  $\mathbf{B}$  in the column space of  $\mathbf{A}$  under the Frobenius norm.

**Low-rank approximation and SVD.** The *singular value decomposition* (SVD) of a matrix  $\mathbf{D} \in \mathbb{R}^{n \times m}$  is given by  $\mathbf{D} = \mathbf{U} \mathbf{\Sigma} \mathbf{V}^T$ , where  $\mathbf{U} \in \mathbb{R}^{n \times n}$  and  $\mathbf{V} \in \mathbb{R}^{m \times m}$  are unitary matrices, and  $\mathbf{\Sigma} \in \mathbb{R}^{n \times m}$  is a diagonal matrix with singular values  $\{\sigma_1, \sigma_2 \dots \sigma_{\min\{n, m\}}\}$  as diagonal entries, conventionally sorted in decreasing order. If the matrix is not clear from the context, we denote as  $\sigma_i(\mathbf{X})$  the  $i$ -th singular value of  $\mathbf{X}$ .

It is known that the optimal rank- $k$  approximation of  $\mathbf{D}$  for the Frobenius and the spectral norm (but not for the max norm) is obtained from the SVD by retaining the first  $k$  singular values, along with the associated  $k$  columns of  $\mathbf{U}$  and  $k$  rows of  $\mathbf{V}^T$  [14]. The largest singular value of a matrix equals its spectral norm, and the number of non-zero singular values indicates the rank of the matrix. As real-world data are often noisy, the singular values are seldom exactly zero. Accordingly, to measure the proximity of a matrix to rank 1, in this work, we use the *low-rankness score* [7], which is given by  $\ell r(\mathbf{X}) = \frac{\sigma_1(\mathbf{X})^2}{\sum_{i=1}^{\min\{n, m\}} \sigma_i(\mathbf{X})^2}$ . A matrix whose singular values after the  $k$ -th one are close to zero can be accurately approximated by a rank- $k$  matrix, and is loosely referred to as *near-rank- $k$*  matrix.

## 4 Problem Formulation

Next, we formalize the problems we study in this paper. To provide better insight, we first present a special case, and then introduce the more general problems.

**Searching for a near-rank-1 subset of rows or columns.** As a warm-up, we introduce a simpler problem that fixes the matrix columns or rows. In other words, in this simplified scenario, we are not looking for arbitrary submatrices, but for submatrices that include all rows or all columns of the input matrix.

*Problem 1 (Largest near-rank-1 subset of rows (LNROSR)).* Given a matrix  $\mathbf{D} \in \mathbb{R}^{n \times m}$  with set of rows  $\mathcal{R}$  and a threshold  $\epsilon \in \mathbb{R}^+$ , find the largest subset of rows  $\mathcal{R}' \subseteq \mathcal{R}$  such that there exist a rank-1 matrix  $\hat{\mathbf{X}} \propto \mathbf{x} \mathbf{y}^T$ , where  $\mathbf{y}^T \in \mathbb{R}^m$  is a row of  $\mathbf{D}$ , satisfying

$$\|\mathbf{D}_{i,:} - \hat{\mathbf{X}}_{i,:}\|_2 \leq \epsilon, \quad \text{for all } i \in \mathcal{R}'. \quad (1)$$

Problem 1 asks to find the largest near-rank-1 submatrix defined over a subset of rows of  $\mathbf{D}$  and all columns. This problem is computationally tractable.

**Proposition 1.** *The LNROSR problem can be solved in polynomial time.*

The proof, via a simple algorithm, is presented in Appendix A.

While Problem 1 asks for a subset of rows, the symmetric problem asking for a subset of columns can be solved simply by considering  $\mathbf{D}^T$  in place of  $\mathbf{D}$ .

**Searching for a near-rank-1 submatrix.** Next, we discuss the more challenging problem of finding a near-rank-1 submatrix, without fixing neither the rows nor the columns of the input matrix.

*Problem 2 (Largest near-rank-1 submatrix (LNROS)).* Given a matrix  $\mathbf{D} \in \mathbb{R}^{n \times m}$ , and a threshold  $\epsilon \in \mathbb{R}^+$ , find a submatrix  $\mathbf{X} \in \mathbb{R}^{n' \times m'}$  of maximum size such that there exist a rank-1 matrix  $\hat{\mathbf{X}}$  satisfying

$$\|\mathbf{E}_{\mathbf{X}, \hat{\mathbf{X}}}\|_* = \|\mathbf{X} - \hat{\mathbf{X}}\|_* \leq \epsilon, \text{ where } * \text{ can be any of the norms } \{F, 2, \max\}. \quad (2)$$

Unfortunately, due to the interaction between rows and columns, the LNROS problem is computationally intractable.

**Proposition 2.** *The LNROS problem is **NP**-hard.*

The **NP**-hardness of LNROS follows from that of the largest rank-1 submatrix problem [10] by setting  $\epsilon = 0$ , and highlights the connection with the *maximum-edge biclique* problem [22], which is made evident in Section 5.

**Searching for a near-rank- $k$  submatrix.** We generalize the LNROS problem to the case of near-rank- $k$  submatrices.

*Problem 3 (Largest near-rank- $k$  submatrix (LN $Rk$ S)).* Given a matrix  $\mathbf{D} \in \mathbb{R}^{n \times m}$ , and a threshold  $\epsilon \in \mathbb{R}^+$ , find a submatrix  $\mathbf{X} \in \mathbb{R}^{n' \times m'}$  of maximum size such that there exist a rank- $k$  matrix  $\hat{\mathbf{X}}$  satisfying

$$\|\mathbf{X} - \hat{\mathbf{X}}\|_* \leq \epsilon, \text{ where } * \text{ can be any of the norms } \{F, 2, \max\}. \quad (3)$$

As LN $Rk$ S is a generalization of LNROS, the LN $Rk$ S problem is also **NP**-hard.

**Extensions.** The problem formulations presented above focus on extracting a single submatrix. In practice, one may wish to find a representation of the input matrix as a sum of  $N$  local low-rank patterns. Such a problem is a generalization of both LNROS and LN $Rk$ S, and hence, inherits their hardness.

Additionally, it may be of interest to identify submatrices that define affine subspaces. Extending our problem formulations and method to the case of affine subspaces (or near-low-rank submatrices up to a particular translation) is straightforward. The details are deferred to an extended version of this work.

## 5 Algorithms

In this section, we present SAMPLEANDEXPAND, our method for discovering near-low-rank submatrices. We first give an overview of the method, and then we present the algorithms to detect near-rank-1 and near-rank- $k$  submatrices.

**Algorithm 1** Overview of SAMPLEANDEXPAND.

---

```

1: Input: Matrix  $\mathbf{D}$ , target rank  $k$ , number of initializations  $N_{init}$ , initial tolerance
    $\delta_{init}$ , tolerance  $\delta$ .
2: Output: Near-rank- $k$  submatrix  $\mathbf{X}^*$ .
3:  $\mathbf{X}^* \leftarrow \mathbf{0}$ 
4: for  $i = 1$  to  $N_{init}$  do
5:    $\mathbf{P} \leftarrow \text{Initialization}(\mathbf{D}, k, \delta_{init})$            // first phase: initialization (sampling)
6:    $\mathbf{X} \leftarrow \text{Expansion}(\mathbf{P}, k, \delta)$            // second phase: expansion
7:   if  $f(\mathbf{X}) \geq f(\mathbf{X}^*)$  then
8:      $\mathbf{X}^* \leftarrow \mathbf{X}$            // select the best submatrix across different initializations
9:   end if
10: end for
11: Return  $\mathbf{X}^*$ 

```

---

### 5.1 High-level Overview of the Method

SAMPLEANDEXPAND is based on a simple two-phase procedure. The first phase *samples* small seed submatrices, and the second phase *expands* those seed submatrices into larger near-low-rank submatrices.

The main idea relies on the simple principle that any submatrix of a rank- $k$  matrix must also have rank at most  $k$ . Thereby, a near-rank-1 submatrix  $\mathbf{X}$  of size  $n' \times m'$  contains a large number of  $2 \times 2$  near-rank-1 submatrices. Thus, if we are looking for a rank-1 submatrix, in the first phase (initialization or sampling phase) we identify a *seed*, which is a  $2 \times 2$  submatrix that can be expanded into a larger submatrix that is still close to a rank-1 approximation. The goal of the second phase (or expansion phase) is to expand the seed into a large near-rank-1 submatrix. Similarly, if we are looking for a near-rank- $k$  submatrix, in the first phase we identify a seed submatrix of minimal size that is close to rank  $k$ . In the second phase, the seed is expanded as much as possible while preserving the proximity to rank  $k$ .

The two-phase procedure is repeated  $N_{init}$  times, to explore different random initializations. Each repetition outputs a near-low-rank submatrix  $\mathbf{X}$ . SAMPLEANDEXPAND accepts a parameter  $\delta$  that controls the trade-off between proximity to a low-rank approximation and size of the output matrices. Higher values of  $\delta$  tend to yield submatrices that are larger but deviate more from a low-rank structure.

After the last repetition, we return the submatrix  $\mathbf{X}$  that maximizes the objective function  $f(\mathbf{X}) = |\mathbf{X}| - \frac{\lambda}{|\mathbf{X}|} \|\mathbf{E}_{\mathbf{X}, \hat{\mathbf{X}}}\|_F^2$ . By default, in the absence of prior information, we standardize the error term and the size, and set  $\lambda = 1$ . However, SAMPLEANDEXPAND is flexible and supports any objective function.

The high-level pseudocode of the SAMPLEANDEXPAND method is given in Algorithm 1. The details of the initialization and expansion phase of the method for the algorithm specialized to near-rank-1 submatrix detection and for the algorithm for general near-rank- $k$  submatrix detection, described later, are different.

**Algorithm 2** Iterative algorithm to find multiple near-rank- $k$  submatrices.

---

```

1: Input: Matrix  $\mathbf{D}$ , vector of target ranks  $\mathbf{k} \in \mathbb{R}^{n \times m}$ , number of initializations  $N_{init}$ ,  

   number of near-low-rank submatrices  $N_{patterns}$ , initial tolerance  $\delta_{init}$ , tolerance  $\delta$ .
2: Output: Estimate  $\hat{\mathbf{D}}$  of  $\mathbf{D}$ .
3:  $\hat{\mathbf{D}} \leftarrow \mathbf{0}$ 
4: for  $h = 1$  to  $N_{patterns}$  do
5:    $\hat{\mathbf{X}}_h \leftarrow \mathbf{0}, \mathcal{R}_h \leftarrow \emptyset, \mathcal{C}_h \leftarrow \emptyset$            // initialize best submatrix across target ranks
6:   for  $k \in \mathbf{k}$  do
7:      $\mathbf{X}, \hat{\mathbf{X}}, \mathcal{R}, \mathcal{C} \leftarrow \text{FINDNEARLOWRANKSUBMATRIX}(\mathbf{D}, k, N_{init}, \delta_{init}, \delta)$  // return
       a near-rank- $k$  submatrix with its rank- $k$  estimate, row and column indices
8:     if  $f(\hat{\mathbf{X}}) > f(\hat{\mathbf{X}}_h)$  then
9:        $\hat{\mathbf{X}}_h \leftarrow \hat{\mathbf{X}}, \mathcal{R}_h \leftarrow \mathcal{R}, \mathcal{C}_h \leftarrow \mathcal{C}$  // update best submatrix across target ranks
10:    end if
11:   end for
12:    $\hat{\mathbf{D}}_{\mathcal{R}_h, \mathcal{C}_h} = \hat{\mathbf{D}}_{\mathcal{R}_h, \mathcal{C}_h} + \hat{\mathbf{X}}_h$            // update current estimate
13:    $\mathbf{D}_{\mathcal{R}_h, \mathcal{C}_h} \leftarrow \mathbf{D}_{\mathcal{R}_h, \mathcal{C}_h} - \hat{\mathbf{X}}_h$            // update input for the next iteration
14: end for
15: Return  $\hat{\mathbf{D}}$ 

```

---

**Approximating the discovered submatrices.** The discovered submatrices can be approximated via SVD. Further, SAMPLEANDEXPAND also naturally leads to a low-rank approximation that is more interpretable than the SVD since it is based on the rows (or columns) of  $\mathbf{X}$ . For the rank-1 case, this approximation is given by  $\hat{\mathbf{X}} = \mathbf{x}\mathbf{y}^T$ , where, either  $\mathbf{y}^T$  is a row or  $\mathbf{x}$  a column of  $\mathbf{X}$ . If, e.g.,  $\mathbf{y}^T$  is a row of  $\mathbf{X}$ ,  $\mathbf{x}$  can be chosen to minimize  $\|\mathbf{X} - \mathbf{x}\mathbf{y}^T\|_F^2$ . The resulting optimal  $\mathbf{x}$  is the vector of coefficients that describe the orthogonal projections of the rows of  $\mathbf{X}$  onto  $\mathbf{y}^T$ . An analogous argument also applies to the columns. As discussed in Section 6, this approximation is supported by quality guarantees.

Although the rank-1 SVD may be more accurate than the interpretable alternative, if a matrix is sufficiently close to rank 1, the difference is typically negligible. To gain some intuition for this claim, note that a matrix that has exactly rank 1 can be represented with no error not only by the discussed interpretable approximation, but also by the rescaled outer product  $\alpha \mathbf{X}_{:,j} \mathbf{X}_{i,:}^T$  of any of its rows and columns, for some  $\alpha \in \mathbb{R}$ . If instead the matrix deviates significantly from rank 1, the rank- $k$  interpretable approximation based on orthogonal projections is often not as accurate as the rank- $k$  SVD.

**Discovering multiple submatrices.** In practice, we may wish to discover multiple submatrices within a single matrix  $\mathbf{D}$  and eventually obtain an approximation  $\hat{\mathbf{D}}$  of the matrix as sum of local low-rank patterns. To achieve this, we run SAMPLEANDEXPAND iteratively. In each iteration, the method finds a single near-rank- $k$  submatrix, and then updates  $\hat{\mathbf{D}}$  and the input matrix for the next iteration. This simple procedure is summarized in Algorithm 2.

**Algorithm 3** Algorithm to find a near rank-1 submatrix.

---

1: **Input:** Matrix  $\mathbf{D} \in \mathbb{R}^{n \times m}$ , number of initializations  $N_{init}$ , initial tolerance  $\delta_{init}$ , tolerance  $\delta$ .  
 2: **Output:** Near-rank-1 submatrix  $\mathbf{X}^*$ .  
 3:  $\mathbf{X}^* \leftarrow \mathbf{0}$  *// start initialization phase*  
 4:  $\Omega \leftarrow \{(i, j)\}, \forall i \in \{1, \dots, n\}, \forall j \in \{1, \dots, m\}$   
 5: **for**  $t = 1$  to  $N_{init}$  **do**  
 6:    $\Gamma' \leftarrow \{(i_1, j_1), (i_2, j_2) \sim Uniform(\Omega)\}$  *// sample two entries at random*  
 7:    $\Gamma \leftarrow \Gamma' \cup \{(i_2, j_1), (i_1, j_2)\}$  *// complete 2 × 2 submatrix*  
 8:    $\mathbf{P}'_{i_h, j_h} \leftarrow \mathbf{D}_{i_h, j_h}, \forall (i_h, j_h) \in \Gamma$   
 9:   **while**  $|\det(\mathbf{P}')| > \delta_{init}$  **do**  
 10:      $\Gamma' \leftarrow \{(i_1, j_1), (i_2, j_2) \sim Uniform(\Omega)\}$  *// repeat until  $\mathbf{P}'$  is close to rank 1*  
 11:      $\Gamma \leftarrow \Gamma' \cup \{(i_2, j_1), (i_1, j_2)\}$   
 12:      $\mathbf{P}'_{i_h, j_h} \leftarrow \mathbf{D}_{i_h, j_h}, \forall (i_h, j_h) \in \Gamma$   
 13:   **end while**  
 14:    $\mathbf{P} \leftarrow \mathbf{P}'$  *// start expansion phase*  
 15:    $(i_a, j_a) \sim Uniform(\Gamma)$  *// select anchor*  
 16:    $(\mathbf{x}^r, \mathbf{x}^c) \leftarrow (\mathbf{D}_{i_a, :}, \mathbf{D}_{:, j_a})$   
 17:    $\mathbf{R}_{i, j}^r \leftarrow \frac{\mathbf{D}_{i, j}}{\mathbf{x}_j^r}, \forall i \in \{1, \dots, n\}, \forall j \in \{1, \dots, m\}$  *// compute row-wise ratios*  
 18:    $\mathbf{R}_{i, j}^c \leftarrow \frac{\mathbf{D}_{i, j}}{\mathbf{x}_i^c}, \forall i \in \{1, \dots, n\}, \forall j \in \{1, \dots, m\}$  *// compute column-wise ratios*  
 19:    $\mathbf{I}^r \leftarrow \mathbf{0}$  *// compute indicator matrix for the rows*  
 20:   **for**  $i = 1$  to  $n$  **do**  
 21:      $\Psi_i \leftarrow \arg \max_{\{\Psi \subseteq \{1, \dots, m\} | j_a \in \Psi, |\mathbf{R}_{i, j_1}^r - \mathbf{R}_{i, j_2}^r| \leq \delta \forall j_1, j_2 \in \Psi\}} |\Psi|$   
 22:      $\mathbf{I}_{i, \Psi_i}^r \leftarrow 1$   
 23:   **end for**  
 24:    $\mathbf{I}^c \leftarrow \mathbf{0}$  *// compute indicator matrix for the columns*  
 25:   **for**  $j = 1$  to  $m$  **do**  
 26:      $\Psi_j \leftarrow \arg \max_{\{\Psi \subseteq \{1, \dots, n\} | i_a \in \Psi, |\mathbf{R}_{i_1, j}^c - \mathbf{R}_{i_2, j}^c| \leq \delta \forall i_1, i_2 \in \Psi\}} |\Psi|$   
 27:      $\mathbf{I}_{\Psi_j, j}^c \leftarrow 1$   
 28:   **end for**  
 29:    $\mathbf{I} \leftarrow \mathbf{I}^r \cap \mathbf{I}^c$  *// compute indicator matrix*  
 30:    $\mathbf{X} \leftarrow \text{EXTRACTMAXIMUMEDGECLIQUE}(\mathbf{I})$   
 31:   **if**  $f(\mathbf{X}) > f(\mathbf{X}^*)$  **then**  
 32:      $\mathbf{X}^* \leftarrow \mathbf{X}$   
 33:   **end if**  
 34: **end for**  
 35: **Return**  $\mathbf{X}^*$

---

## 5.2 Recovering a Near-rank-1 Submatrix

Here, we present the initialization (sampling) and expansion phases of the algorithm to discover near-rank-1 submatrices. Algorithm 3 presents the pseudocode.

**Initialization.** To find the initial  $2 \times 2$  near-rank-1 submatrix  $\mathbf{P}$ , we sample two distinct row indices  $\{i_1, i_2\}$  and column indices  $\{j_1, j_2\}$  of the input matrix  $\mathbf{D}$ , and then we compute the determinant of the associated  $2 \times 2$  submatrix  $\mathbf{P}'$ :

$$|\det(\mathbf{P}')| = |\mathbf{D}_{i_1, j_1} \mathbf{D}_{i_2, j_2} - \mathbf{D}_{i_1, j_2} \mathbf{D}_{i_2, j_1}|.$$

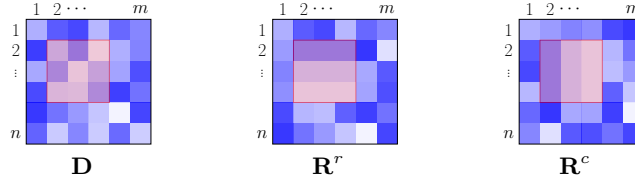


Fig. 3: Example of row-wise ( $\mathbf{R}^r$ ) and column-wise ( $\mathbf{R}^c$ ) ratio matrices associated with an input matrix ( $\mathbf{D}$ ) containing a rank-1 submatrix (highlighted in red). Within this rank-1 submatrix, the entries of  $\mathbf{R}^r$  are constant across rows, and the entries of  $\mathbf{R}^c$  are constant across columns.

If  $|\det(\mathbf{P}')| \leq \delta_{init}$ , for some input  $\delta_{init} \in \mathbb{R}^+$ ,  $\mathbf{P}'$  is close to rank 1, and hence it may be contained into a larger near-rank-1 submatrix. Therefore,  $\mathbf{P}'$  is the seed  $\mathbf{P}$  that will be expanded. If instead  $|\det(\mathbf{P}')| > \delta_{init}$ , we sample different  $2 \times 2$  submatrices  $\mathbf{P}'$  until we find a seed to expand. In practice,  $\delta_{init}$  is initialized to a small value ( $10^{-11}$  by default) and progressively increased until the seed is found.

**Expansion.** To extend  $\mathbf{P}$  into a larger submatrix, we consider one of the entries  $(i_a, j_a)$  in  $\mathbf{P}$ , which we call *anchor*. Then, we divide all rows in  $\mathbf{D}$  by the  $i_a$ -th row, obtaining the row-wise ratio matrix  $\mathbf{R}^r$  and all columns by the  $j_a$ -th column, obtaining the column-wise ratio matrix  $\mathbf{R}^c$ . If an entry in the  $i_a$ -th row or  $j_a$ -th column of  $\mathbf{D}$  is zero, we add a small positive constant to prevent division by zero.

As illustrated in Figure 3, if the matrix  $\mathbf{D}$  contains a submatrix  $\mathbf{X}$  of rank 1, the entries corresponding to  $\mathbf{X}$  in  $\mathbf{R}^r$  and  $\mathbf{R}^c$  will be row-wise and column-wise constant, respectively. More generally, as we explain in Section 6, bounding the variation in all the row-wise and column-wise ratios in a submatrix leads to quality guarantees for its rank-1 approximation. Therefore, the goal of the expansion stage is to identify a submatrix of maximum size with bounded variation in the row-wise and column-wise ratios.

To this end, our algorithm examines the rows of  $\mathbf{R}^r$  to find subsets of near-constant entries including column  $j_a$  and the columns of  $\mathbf{R}^c$  to find subset of near-constant entries including row  $i_a$ . More specifically, for an input parameter  $\delta \in \mathbb{R}^+$ , we select, for each row of  $\mathbf{R}^r$ , the  $j_a$ -th entry and all other entries such that the maximum variation is less than  $\delta$  in absolute value. Similarly, for each column of  $\mathbf{R}^c$ , we select the  $i_a$ -th entry and all other entries such that the maximum variation is less than  $\delta$  in absolute value. Subsets within each row can be efficiently retrieved by sorting the row elements by their absolute deviation from the  $j_a$ -th element and analogously for the columns.

Given the identified subsets, we construct two indicator matrices:  $\mathbf{I}^r \in \{0, 1\}^{n \times m}$ , where the entries with value 1 correspond to subsets of near-constant row-wise ratios; and  $\mathbf{I}^c \in \{0, 1\}^{n \times m}$ , where the entries with value 1 correspond to subsets of near-constant column-wise ratios. We can then compute the intersection of the two matrices  $\mathbf{I}^r$  and  $\mathbf{I}^c$  to obtain the intersection indicator matrix  $\mathbf{I}$  of the same dimensions. The problem of extracting a submatrix of maximum size with all row-wise and column-wise ratios with bounded variations can then be framed

as the problem of finding the largest possible all-ones submatrix within  $\mathbf{I}$ . This problem is equivalent to the extraction of a maximum-edge biclique [22] from the bipartite graph  $\mathcal{G}_{\mathbf{I}}$  that has  $\mathbf{I}$  as adjacency matrix. Although this is an **NP**-hard problem [22], so that it cannot be solved in polynomial time, we can leverage recent algorithmic advances that solve the problem quickly in considerably dense and large bipartite graphs [22]. In addition, to avoid possible scalability issues that may still arise, we also rely on effective heuristics, as discussed in Section 5.4.

### 5.3 Recovering a Near-rank- $k$ Submatrix

Next, we illustrate the adaptation of the initialization (sampling) and expansion phases of **SAMPLEANDEXPAND** to the general case of recovery of near-rank- $k$  submatrices. The pseudocode is given in Algorithm 4.

**Initialization.** To find a seed, that is, a minimal near-rank- $k$  submatrix, we sample matrices with  $k + 1$  rows and columns until we find a matrix  $\mathbf{P}$  that, as indicated by a near-zero determinant, is close to rank  $k$  or lower, and thus represents the seed to expand in the second phase. In particular, to determine whether a matrix  $\mathbf{P}'$  has rank  $k$  or lower, we check whether  $|\det(\mathbf{P}')| \leq \delta_{init}$ , for a small  $\delta_{init} \in \mathbb{R}^+$ , which, as for the algorithm tailored to near-rank-1 submatrices, is first initialized to a to a small value and then increased until a seed  $\mathbf{P}$  is found.

**Expansion.** Given the seed matrix  $\mathbf{P} \in \mathbb{R}^{k+1,k+1}$ , of rank  $k' \leq k$ , we sample  $k'$  anchor rows from the rows of  $\mathbf{P}$ . Let  $\mathcal{C}_{\mathbf{P}}$  denote the set of the  $k + 1$  indices of the columns in  $\mathbf{P}$ . Considering only the columns in  $\mathcal{C}_{\mathbf{P}}$ , we compute the coefficients of the orthogonal projection of each row of  $\mathbf{D}$  onto the subspace spanned by the  $k'$  anchor rows.

We then compute the matrix of orthogonal projections  $\hat{\mathbf{D}}^\perp \in \mathbb{R}^{n \times m}$  expressing each row as a linear combination of the anchor rows with weights given by the orthogonal-projection coefficients. The coefficients are obtained by considering only the columns in  $\mathcal{C}_{\mathbf{P}}$ , identified in the initialization phase. Nevertheless, the matrix  $\hat{\mathbf{D}}^\perp \in \mathbb{R}^{n \times m}$ , similarly to the ratio matrices in the rank-1 case, indicates which additional columns and rows are close to a rank- $k$  approximation. More specifically, all entries  $\mathbf{D}_{i,j}$  that are closely approximated by  $\hat{\mathbf{D}}_{i,j}^\perp$  lie close to the  $k$ -dimensional subspace identified in the initialization phase.

Therefore, to find a near-rank- $k$  submatrix of maximum size, we need to identify the largest submatrix of  $\hat{\mathbf{D}}_{i,j}^\perp$  where all entries nearly match the corresponding entries of  $\mathbf{D}$ . To obtain such a submatrix, we calculate the matrix of absolute errors  $\mathbf{E}^{abs} = |\mathbf{D} - \hat{\mathbf{D}}^\perp|$ , and from it, the indicator matrix  $\mathbf{I}^r$ , which takes value 1 for entry  $(i, j)$  if  $\mathbf{E}_{i,j}^{abs} \leq \delta$  and 0 otherwise, for some input  $\delta \in \mathbb{R}^+$ . Figure 4 presents an example of the matrices  $\hat{\mathbf{D}}^\perp$  and  $\mathbf{E}^{abs}$ .

The same procedure followed to determine  $\mathbf{I}^r$ , but on input  $\mathbf{D}^T$  and  $\mathbf{P}^T$  yields  $\mathbf{I}^c$ . Similarly to the case of near-rank-1 submatrix discovery, the intersection of  $\mathbf{I}^r$  and  $\mathbf{I}^{cT}$  gives the matrix  $\mathbf{I}$  and the associated bipartite graph  $\mathcal{G}_{\mathbf{I}}$ . The desired output near-rank- $k$  submatrix is then given by a submatrix of  $\mathbf{I}$  consisting of all ones, or, equivalently, by a maximum-edge biclique of  $\mathcal{G}_{\mathbf{I}}$ .

**Algorithm 4** Algorithm to find a near-rank- $k$  submatrix.

---

1: **Input:** Matrix  $\mathbf{D} \in \mathbb{R}^{n \times m}$ , target rank  $k$ , number of initializations  $N_{init}$ , initial tolerance  $\delta_{init}$ , tolerance  $\delta$ .  
 2: **Output:** Near-rank- $k$  submatrix  $\mathbf{X}^*$ .  
 3:  $\mathbf{X}^* \leftarrow \mathbf{0}$  *// start initialization phase*  
 4:  $\Omega \leftarrow \{(i, j)\}, \forall i \in \{1, \dots, n\}, \forall j \in \{1, \dots, m\}$   
 5: **for**  $t = 1$  to  $N_{init}$  **do**  
 6:    $\Gamma \leftarrow \{(i_h, j_h) \sim Uniform(\Omega) \mid h = 1, \dots, k + 1\}$   
 7:    $\mathbf{P}'_{i_h, j_h} \leftarrow \mathbf{D}_{i_h, j_h}, \forall (i_h, j_h) \in \Gamma$   
 8:   **while**  $|\det(\mathbf{P}')| > \delta_{init}$  **do**  
 9:      $\Gamma \leftarrow \{(i_h, j_h) \sim Uniform(\Omega) \mid h = 1, \dots, k + 1\}$   
 10:     $\mathbf{P}'_{i_h, j_h} \leftarrow \mathbf{D}_{i_h, j_h}, \forall (i_h, j_h) \in \Gamma$  *// repeat until  $\mathbf{P}'$  is rank-deficient*  
 11:   **end while**  
 12:    $\mathbf{P} \leftarrow \mathbf{P}'$  *// start expansion phase*  
 13:    $\mathbf{I}^r \leftarrow \text{EXTRACTINDICATORMATRIX}(\mathbf{D}, n, \mathbf{P}, \Gamma, k, \delta)$   
 14:    $\Gamma_C \leftarrow \{(j, i)\}, \forall (i, j) \in \Gamma$   
 15:    $\mathbf{I}^c \leftarrow \text{EXTRACTINDICATORMATRIX}(\mathbf{D}^T, m, \mathbf{P}^T, \Gamma_C, k, \delta)$   
 16:    $\mathbf{I} \leftarrow \mathbf{I}^r \cap \mathbf{I}^{cT}$  *// compute indicator matrix*  
 17:    $\mathbf{X} \leftarrow \text{EXTRACTMAXUMEDGEBICLIQUE}(\mathbf{I})$   
 18:   **if**  $f(\mathbf{X}) > f(\mathbf{X}^*)$  **then**  
 19:      $\mathbf{X}^* \leftarrow \mathbf{X}$   
 20:   **end if**  
 21: **end for**  
 22: **Return**  $\mathbf{X}^*$   
 23: **Procedure** EXTRACTINDICATORMATRIX  
 24: **Input:** Input matrix  $\mathbf{D}^A$ , number of rows  $n^A$ , initial submatrix  $\mathbf{P}^A$ , set of indices  $\Gamma^A$ , target rank  $k$ , tolerance  $\delta$ .  
 25: **Output:** indicator matrix  $\mathbf{I}^A$ .  
 26:  $\Phi \leftarrow \{i_h \sim Uniform(\{1, \dots, n^A\}) \mid h = 1, \dots, k\}$  *// sample  $k$  indices*  
 27:  $\mathbf{C} \leftarrow \mathbf{D}_{:, j; j \in \Gamma^A} \mathbf{P}_{\Phi, :}^+$  *// compute orthogonal-projection coefficients*  
 28:  $\hat{\mathbf{D}}^\perp \leftarrow \mathbf{C} \mathbf{D}_{\Phi, :}$  *// compute orthogonal projections*  
 29:  $\mathbf{E}^{abs} \leftarrow |\hat{\mathbf{D}}^\perp - \mathbf{D}|$  *// compute matrix of absolute errors*  
 30:  $\mathbf{I}^A_{i,j} \leftarrow \mathbf{1}(\mathbf{E}^{abs}_{i,j} \leq \delta)$   
 31: **Return**  $\mathbf{I}^A$

---

#### 5.4 Scalability Considerations

One limitation of SAMPLEANDEXPAND is its reliance on solving the maximum-edge biclique problem, which is **NP-hard**. While the algorithm we use to extract these bicliques is often efficient in practice [22], scalability issues may still arise. To address such issues, the algorithm for finding maximum-edge bicliques can be replaced with a more scalable heuristic. Among many possible different heuristic approaches, by default, we rely on spectral biclustering [19], which is empirically found to be particularly effective in quickly identifying a dense submatrix of  $\mathbf{I}$ . Even more efficient and scalable approaches include algorithms to extract dense bipartite subgraphs, a greedy algorithm removing rows and columns from  $\mathbf{I}$ , e.g., based on the amount of ones, and a randomized algorithm sampling submatrices

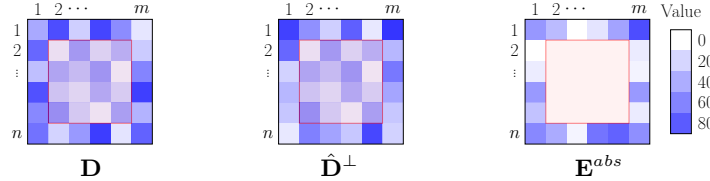


Fig. 4: Example of matrices of projections ( $\hat{\mathbf{D}}^\perp$ ) and absolute errors ( $\mathbf{E}^{abs}$ ) associated with an input matrix ( $\mathbf{D}$ ) containing a rank- $k$  submatrix (highlighted in red). Within this rank- $k$  submatrix, the entries of  $\hat{\mathbf{D}}^\perp$  are equal to those of  $\mathbf{D}$ , and the entries of  $\mathbf{E}^{abs}$  are all identically zero.

from  $\mathbf{I}$  according to the amount of ones they contain [3]. A comprehensive evaluation of the performance of various heuristics for approximating maximum-edge bicliques is left to future work.

## 6 Analysis

In this section, we explain how the proposed methods yield submatrices with bounded approximation error. We also provide a brief discussion on the probabilistic aspects and on the computational complexity of the methods.

### 6.1 Approximation Error Guarantees

In global low-rank approximation, the presence of outliers in the data may lead to situations where the whole matrix cannot be approximated with a low-rank structure without compromising the overall approximation quality. However, as our problem definition lifts the requirement that the whole matrix must be approximated, it is interesting to control the *entry-wise* maximum approximation error in the discovered submatrices. We thus provide approximation-error guarantees in terms of the max norm. A bound on the max norm yields bounds on the Frobenius and spectral norms, albeit loose. In the case of near-rank-1 submatrix discovery, we also provide interesting bounds on the spectral and Frobenius norms that are not a direct consequence of the bound on the max norm.

**Near-rank-1 submatrices.** As mentioned in Section 5.1,  $n' \times m'$  near-rank-1 submatrices contain many near-rank-1  $2 \times 2$  submatrices. Building on this intuition, SAMPLEANDEXPAND starts by locating a  $2 \times 2$  submatrix  $\mathbf{P}$  with bounded determinant, and hence close to rank 1. Then, it computes row-wise and column-wise ratios dividing all rows (columns) by a single anchor row (column) with index sampled from those of  $\mathbf{P}$ , and finds submatrices with rows (columns) of nearly-constant ratios. Nearly-constant ratios correspond to bounded  $2 \times 2$  determinants. For instance, if  $\left| \frac{\mathbf{D}_{i,j_1}}{x_{j_1}^r} - \frac{\mathbf{D}_{i,j_2}}{x_{j_2}^r} \right| \leq \delta$ , where the left-hand side is a difference of ratios, then  $|\mathbf{D}_{i,j_1}x_{j_2}^r - \mathbf{D}_{i,j_2}x_{j_1}^r| \leq \delta|x_{j_1}^r||x_{j_2}^r|$ , where the left-hand side is a  $2 \times 2$  determinant. Bounding the variation of all the ratios within each row and column

of a submatrix, and thus the corresponding  $2 \times 2$  determinants, SAMPLEANDEXPAND yields submatrices composed of  $2 \times 2$  near-rank-1 submatrices, which, as formalized in Theorem 1, results in approximation guarantees.

**Theorem 1.** *Let  $\mathbf{X} \in \mathbb{R}^{n' \times m'}$  be a near-rank-1 submatrix output by SAMPLEANDEXPAND with anchor row  $\mathbf{x}^r$ , anchor column  $\mathbf{x}^c$  and input tolerance  $\delta$ . There exists a rank-1 approximation  $\hat{\mathbf{X}}$  of  $\mathbf{X}$  such that for  $\mathbf{E}_{\mathbf{X}, \hat{\mathbf{X}}} = \mathbf{X} - \hat{\mathbf{X}}$  it holds:*

$$\|\mathbf{E}_{\mathbf{X}, \hat{\mathbf{X}}}\|_{\max} \leq \min \{\delta g_{\max}(\mathbf{x}^r), \delta g_{\max}(\mathbf{x}^c)\}, \quad (4)$$

and

$$\|\mathbf{E}_{\mathbf{X}, \hat{\mathbf{X}}}\|_2 \leq \|\mathbf{E}_{\mathbf{X}, \hat{\mathbf{X}}}\|_F \leq \min \left\{ \delta \sqrt{(n-1)g_F(\mathbf{x}^r)}, \delta \sqrt{(m-1)g_F(\mathbf{x}^c)} \right\}, \quad (5)$$

where  $g_{\max}(\mathbf{x}) = \frac{\max_i |x_i|^3}{2 \min_i x_i^2}$  and  $g_F(\mathbf{x}) = \frac{\sum_{i < j} x_i^2 x_j^2}{\|\mathbf{x}\|_2^2}$ .

Theorem 1 suggests that the low-rank-approximation error incurred by the near-rank-1 submatrices discovered by SAMPLEANDEXPAND can be bounded by a function of the input parameter  $\delta$  and of the scale of  $\mathbf{x}^r$  or  $\mathbf{x}^c$ . Therefore, given the anchor row and column, one can set the value of  $\delta$  to guarantee that the maximum or the total approximation error is bounded by a user-specified threshold  $\epsilon \in \mathbb{R}^+$ , as requested by Problem 2. However, the approximation-error guarantees given in Theorem 1 only hold if SAMPLEANDEXPAND extracts a biclique in the last step. Alternative heuristic approaches that do not extract a biclique can be effective in practice, but they are not supported by approximation-error guarantees.

Notably, the approximation-error guarantees are achieved by the interpretable rank-1 approximation discussed in Section 5.1. In addition, for the rank-1 SVD approximation  $\hat{\mathbf{X}}$ , Theorem 2 in Appendix B bounds the spectral norm of the error  $\mathbf{E}_{\mathbf{X}, \hat{\mathbf{X}}} = \mathbf{X} - \hat{\mathbf{X}}$ .

**Near-rank- $k$  submatrices.** The algorithm for the more general task of identifying near-rank- $k$  submatrices does not admit the same analysis as the algorithm for identifying near-rank-1 submatrices. However, the algorithm for the rank- $k$  case, by design, discovers submatrices  $\mathbf{X}$  such that  $\mathbf{E}_{\mathbf{X}, \hat{\mathbf{X}}} = \mathbf{X} - \hat{\mathbf{X}}$  satisfies  $\|\mathbf{E}_{\mathbf{X}, \hat{\mathbf{X}}}\|_{\max} \leq \delta$ . As mentioned, the bound on the max norm leads to a straightforward bound on the Frobenius and spectral norms, namely  $\|\mathbf{E}_{\mathbf{X}, \hat{\mathbf{X}}}\|_2 \leq \|\mathbf{E}_{\mathbf{X}, \hat{\mathbf{X}}}\|_F \leq \delta \sqrt{(n-k)(m-k)}$ , which can also be used to set the value of  $\delta$  based on a user-specified error threshold  $\epsilon$  on the Frobenius or spectral norm.

## 6.2 Probabilistic Analysis

In this section, we discuss simple probabilistic aspects of our method.

**Probability of discovering a near-rank-1 submatrix.** Let  $\mathbf{X}$  be a target near-rank-1 submatrix of size  $|\mathbf{X}|$  within  $\mathbf{D} \in \mathbb{R}^{n \times m}$ . The probability that SAMPLEANDEXPAND discovers  $\mathbf{X}$  by one sample is  $p = \frac{|\mathbf{X}|}{nm} \frac{|\mathbf{X}|-1}{nm-1}$ . Hence, the probability of discovering  $\mathbf{X}$  in  $N_{init}$  iterations is  $1 - (1-p)^{N_{init}}$ , and therefore the number of

iterations required to discover  $\mathbf{X}$  with probability at least  $\alpha_p$  is  $N_{init} \geq \frac{\ln(1-\alpha_p)}{\ln(1-p)}$ . For instance, if  $p = 0.1$  and  $\alpha_p = 0.9$ , we need  $N_{init} > \frac{\ln(1-0.9)}{\ln(1-0.1)} \approx 22$  iterations.

Basic probability theory implies that, in expectation, the number of iterations necessary to discover  $\mathbf{X}$  is  $\frac{1}{p}$ , and we discover it  $pN_{init}$  times in  $N_{init}$  iterations.

**Probability of discovering a near-rank-k submatrix.** The simple probabilistic analysis presented above for near-rank-1 submatrices also applies to near-rank- $k$  submatrices. The only difference is that, in this case, we have  $p = \frac{|\mathbf{X}|}{nm} \frac{|\mathbf{X}|-1}{nm} \dots \frac{|\mathbf{X}|-k}{nm-k}$ , which can become small as  $k$  grows. Yet, larger values of  $k$  tend to be associated with larger values of  $|\mathbf{X}|$  and, in practice, we are interested in small values of  $k$ .

**Probability of occurrence of a  $2 \times 2$  near-rank-1 matrix.** We conclude the section by investigating the probability with which SAMPLEANDEXPAND identifies a seed  $2 \times 2$  submatrix with near-zero determinant in random matrices. Let  $\mathbf{D}$  be a random matrix with i.i.d. entries distributed according to  $\mathcal{Z}$ , and let  $E(\mathcal{Z}) = \mu$  and  $Var(\mathcal{Z}) = \sigma^2$  be the expectation and variance of  $\mathcal{Z}$ . To study the probability of occurrence of  $2 \times 2$  submatrices with near-zero determinant, we consider the random variable  $\mathcal{W} = x_1y_2 - x_2y_1$ , where  $x_1, x_2, y_1$  and  $y_2$  are the entries of a  $2 \times 2$  submatrix.

By independence,  $E(x_1y_2) = E(x_1)E(y_2)$  and  $Var(x_1y_2) = Var(x_1)Var(y_2) + E(y_2)^2Var(x_1) + E(x_1)^2Var(y_2) = \sigma^4 + 2\mu^2\sigma^2$ , and similarly for  $x_2y_1$ .

Further, since  $x_2y_1$  and  $x_2y_1$  are independent,

$$E(x_1y_2 - x_2y_1) = E(x_1y_2) - E(x_2y_1) = 0 \text{ and} \\ Var(x_1y_2 - x_2y_1) = Var(x_1y_2) + Var(x_2y_1) = 2\sigma^4 + 4\mu^2\sigma^2.$$

Chebyshev's inequality [27] then implies that:

$$P(|\mathcal{W}| \geq \delta_{init}) \leq \frac{2\sigma^4 + 4\mu^2\sigma^2}{\delta_{init}^2},$$

giving a bound on the probability that a  $2 \times 2$ -submatrix deviates significantly from rank 1. The preliminary experiments presented in Appendix E additionally provide an empirical investigation of this probability. Assumptions on  $\mathcal{Z}$  may lead to tighter bounds, a question that we leave open for future work.

### 6.3 Computational Complexity

Finally, we discuss the computational complexity of SAMPLEANDEXPAND.

Consider a single iteration of the method. The runtime bottleneck is due to finding a maximum-edge biclique, which, in the worst case can take exponential time. However, the algorithm introduced by Lyu et al. [22] prunes large portions of the search space and can be very efficient in practice. As discussed in Section 5.4, to improve scalability, we can use a more scalable heuristic for finding an approximate maximum-edge biclique. The spectral biclustering algorithm, which is the heuristic we rely on by default, has computational complexity determined

by the computation of the (truncated) SVD, which is  $\mathcal{O}(\min(n^2m, m^2n))$ . If an even more scalable heuristic is leveraged, such as a basic linear-time algorithm removing rows and columns of  $\mathbf{I}$  with less than a given proportion of ones, SAMPLEANDEXPAND for the rank-1 case and for the general rank- $k$  case incurs computational complexity  $\mathcal{O}(n + m)$  and  $\mathcal{O}(nkm)$ , respectively.

As SAMPLEANDEXPAND generally explores different initializations, if  $\tau$  is the complexity of a single iteration, then  $\mathcal{O}(N_{init}\tau)$  is the overall complexity.

## 7 Experiments

In this section, we evaluate the performance of SAMPLEANDEXPAND against existing approaches. We consider both synthetic data and real-world data. More details on the experimental setup are provided in Appendix D, and additional experimental results are presented in Appendix E.

### 7.1 Experimental Setup

**Datasets.** We conduct experiments on both synthetic and real-world datasets.

The synthetic data are generated by planting near-rank-1 submatrices into larger matrices. To make the discovery task as challenging as possible, the entries of the planted submatrices and of the background are generated from the same distributions. We consider six different distributions. The details of the data-generating mechanisms are given in Appendix D.

Additionally, we consider 15 real-world datasets from different applications, including user ratings, images, and gene-expression data. We report summary characteristics for the real-world datasets in Table 1,

**Baselines.** We compare SAMPLEANDEXPAND against baselines discussed in Section 2. Specifically, we consider a method (CVX) based on convex optimization [10], PCA with sparsity constraints (SPARSEPCA) [24], SVP [26], and RPSP [7]. In the experiments with real data, we restrict the comparison to the most recently introduced methods, SVP and RPSP, which specifically aim at discovering (possibly multiple) near-low-rank submatrices.

**Metrics.** In experiments with synthetic data, all methods output matrices  $\hat{\mathbf{D}}$  that contain low-rank approximations of the identified submatrices and zero entries for all indices that are not part of such submatrices. To measure the ability of a method in recovering the indices of the planted ground-truth submatrices, we report the  $F_1$  score. Based on the same output, we also report the error (squared Frobenius norm averaged over the entries) incurred in approximating the ground-truth submatrices. SAMPLEANDEXPAND approximates submatrices through the interpretable approach discussed in Section 5.1 for  $k = 1$  and via SVD for  $k > 1$ . All baselines approximate submatrices via SVD.

In real-world datasets, where no ground truth is available, we report the size and low-rankness score (introduced in Section 3) of the returned submatrices.

In all cases, we measure runtimes in seconds.

Table 1: Summary characteristics for real-world datasets. We report the number of rows, columns, the low-rankness score, the entry-wise maximum squared deviation from the rank-1 SVD (Max rank-1 deviation) and a reference.

| Dataset       | # Rows | # Columns | Low-rankness score | Max rank-1 deviation | Reference |
|---------------|--------|-----------|--------------------|----------------------|-----------|
| HYPERSPECTRAL | 5 554  | 2 151     | 0.89               | 0.23                 | [21]      |
| ISOLET        | 7797   | 617       | 0.88               | 0.98                 | [2]       |
| OLIVETTI      | 400    | 4096      | 0.95               | 0.53                 | [2]       |
| MOVIELENS     | 943    | 1682      | 0.30               | 1.00                 | [16]      |
| ORL           | 400    | 1024      | 0.95               | 0.55                 | [5]       |
| AL-GENES      | 7129   | 38        | 1.00               | 0.28                 | [11]      |
| MANDRILL      | 512    | 512       | 0.92               | 0.36                 | [28]      |
| OZONE         | 2536   | 72        | 1.00               | 0.08                 | [2]       |
| BRCA-GENES    | 317    | 496       | 0.72               | 0.89                 | [30]      |
| GOOGLE        | 5456   | 24        | 0.76               | 0.77                 | [2]       |
| NPAS          | 1418   | 78        | 0.85               | 0.15                 | [18]      |
| CAMERAMAN     | 256    | 256       | 0.86               | 0.56                 | [28]      |
| MOVIETRUST    | 200    | 200       | 0.77               | 1                    | [18]      |
| HEARTH        | 920    | 15        | 0.94               | 0.08                 | [2]       |
| IMAGENET      | 64     | 27        | 0.92               | 0.22                 | [8]       |

**Parameters.** The important parameter to set for our method is the tolerance  $\delta$  controlling the trade-off between low-rankness and size. As explained in Section 6, one can set  $\delta$  to match an input bound  $\epsilon$  on the allowed low-rank-approximation error. In our experiments, however, we explore few fixed values of  $\delta$ . Specifically, for experiments with synthetic data, we set  $\delta$  to 0.05 and the number of initializations  $N_{init}$  to 25. For experiments with real-world data, we let  $\delta$  vary in  $\{10^{-1}, 10^{-2}, 10^{-3}, 10^{-4}\}$ , and we consider  $N_{init} = 25$  initializations for each value of  $\delta$ . Finally, the initialization parameter  $\delta_{init}$  is set to  $10^{-11}$  and is increased by 10 every 10000 samples that do not result in a submatrix to expand.

**Implementation.** Our Python implementation is available online<sup>4</sup>. Experiments are performed on a computer with  $2 \times 10$  core Xeon E5 processor and 256 GB memory. All reported results are averages over 10 runs.

## 7.2 Experiment Results

We first present results for the experiments in synthetic data and then the results for the experiments in real-world datasets.

**Results on synthetic datasets.** Figure 5 presents results for the task of near-rank-1-submatrix discovery in  $250 \times 250$  matrices of entries generated from six different probability distributions. The results show that our method consistently recovers the ground truth (as indicated by  $F_1$  score close to 1 and reconstruction

<sup>4</sup> <https://github.com/maciap/SaE>

error close to 0), which is not the case for the baseline approaches. More specifically, RPSP tends to recover the ground-truth submatrix as its size increases, but it is also considerably slower than the other methods. SPARSEPCA and SVP are the fastest algorithms, but, like CVX, they often fail in detecting the ground truth.

We also observe significant variability in the results associated with different data-generating distributions. In particular, as suggested by Figure 5, the only case where SAMPLEANDEXPAND does not achieve an average  $F_1$  score close to 1 in near-rank-1 submatrix recovery is for Poisson-distributed data with a planted near-rank-1 submatrix accounting for the 10% percent of the total amount of entries. The synthetic data are not scaled in preprocessing. Thus, it is possible that the  $F_1$  score would approach 1 also in this case after suitably adjusting the parameter  $\delta$  input to SAMPLEANDEXPAND or normalizing the input matrix  $\mathbf{D}$ .

Figure 6 shows the same metrics as in Figure 5, for synthetic data with entries generated from the same probability distributions, but in the setting where multiple, possibly overlapping, near-rank-1 submatrices are planted and discovered. The results in this more challenging setting highlight that SAMPLE-ANDEXPAND is the only method that consistently retrieves the ground-truth submatrices. Among the baselines, SPARSEPCA stands out for its accurate reconstruction. However, the estimate  $\hat{\mathbf{D}}$  of the input matrix it generates quickly becomes very dense as more submatrices are discovered, and hence this approach fails to identify the locations of the ground-truth submatrices.

Finally, Figure 10 in Appendix E demonstrates the robustness of our method with respect to noise.

**Results on real-world data.** Table 2 reports low-rankness score and size averaged over the top-5 submatrices retrieved by our method, SVP and RPSP in real-world datasets. To determine the top-5 submatrices returned by each method, we select those that maximize the minimum between the low-rankness score and the size. Moreover, to offer a more complete picture, in the appendix (Figure 11), we additionally display the low-rankness and size of the individual top-5 patterns.

Finding submatrices with high low-rankness is not an easy task. SVP returns large submatrices. However, those submatrices usually have smaller low-rankness compared to those discovered by our method and RPSP, and, in several cases, compared to the input matrix. SAMPLEANDEXPAND and RPSP are more likely than SVP to return submatrices with large low-rankness. Furthermore, SAMPLE-ANDEXPAND tends to discover submatrices that strike a more desirable balance between low-rankness and size compared to RPSP.

As concerns runtime, SAMPLEANDEXPAND is drastically faster than RPSP in smaller datasets, but it can become slower in larger datasets. Nonetheless, the runtime of our method could be significantly reduced by leveraging a more efficient approach to maximum-edge-biclique extraction and by reducing the number of iterations, which, however, could deteriorate the quality of the results. As mentioned in Section 5.4, future work will study the performance of different heuristic approaches to maximum-edge-biclique extraction in terms of quality of the results, efficiency and scalability.

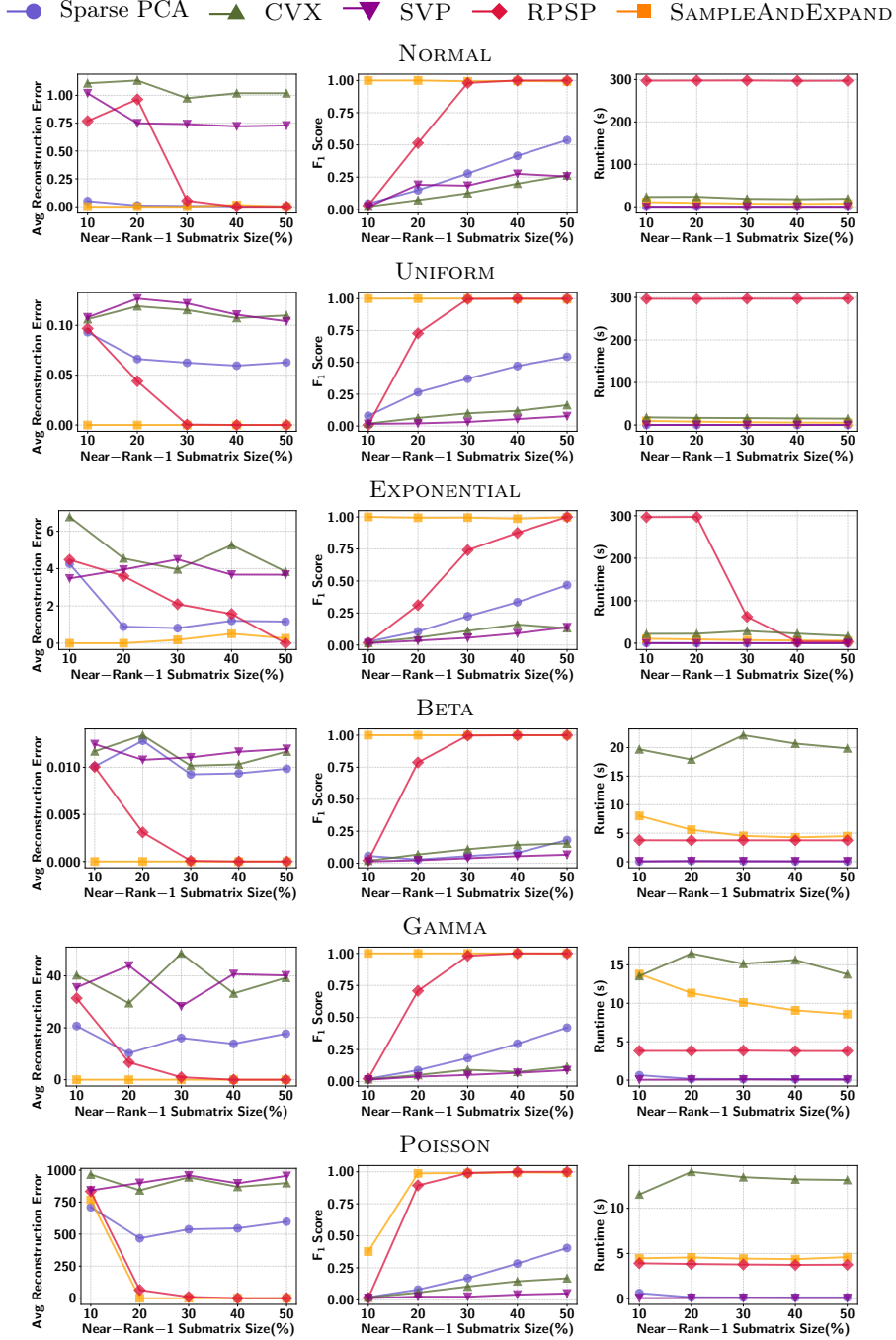


Fig. 5: Full-rank synthetic  $250 \times 250$  matrices generated from different probability distributions with a planted near-rank-1 submatrix. Performance of different methods in the task of near-rank-1 submatrix discovery. We show the average (per-entry) reconstruction error (left), the  $F_1$  score (center) and the runtime (right) of different methods as a function of planted submatrix size.

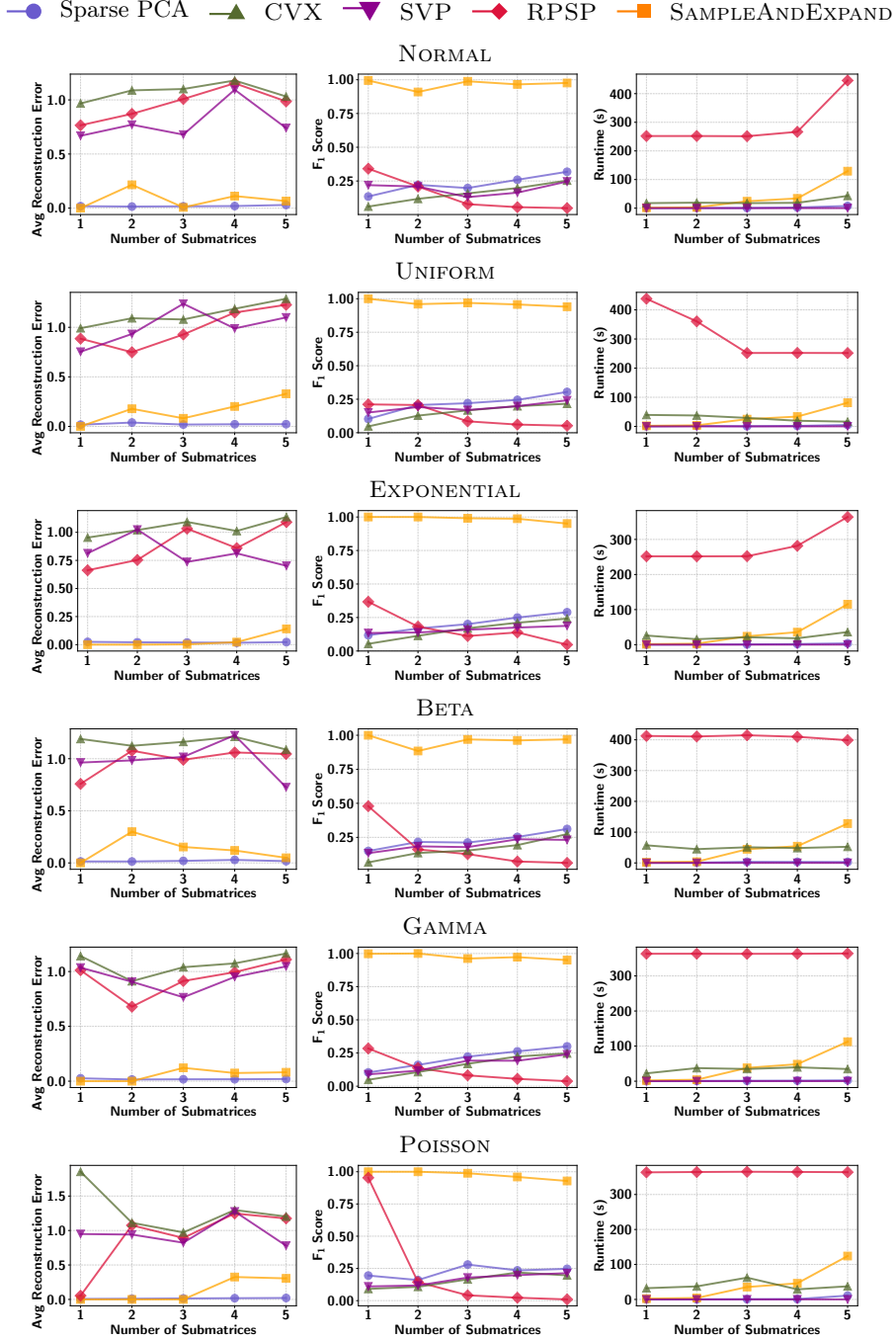


Fig. 6: Full-rank synthetic  $250 \times 250$  matrices generated from different probability distributions with multiple (possibly overlapping) planted near-rank-1 submatrices. Performance of different methods in discovering planted submatrices. We show the average (per-entry) reconstruction error (left), the  $F_1$  score (center) and the runtime (s) as a function of the number of planted submatrices.

Table 2: Performance in real-world data. For the top 5 local low-rank patterns identified by the methods, we show the average relative percentage increase (L-R) with respect to the low-rankness score of the input matrix, the size (in percentage of entries of the input matrix) and the runtime (in seconds) to obtain them.

| Dataset       | SVP    |       |         | RPSP   |      |         | SAMPLEANDEXPAND |       |         |
|---------------|--------|-------|---------|--------|------|---------|-----------------|-------|---------|
|               | L-R    | Size  | Runtime | L-R    | Size | Runtime | L-R             | Size  | Runtime |
| HYPERSPECTRAL | 4.05   | 2.88  | 47.0    | 9.84   | 2.10 | 590     | 11.09           | 21.43 | 1697    |
| ISOLET        | -8.08  | 3.21  | 11      | 4.06   | 3.51 | 409     | 7.08            | 9.9   | 650     |
| OLIVETTI      | -1.39  | 4.3   | 3       | 2.23   | 2.81 | 366     | 3.83            | 5.2   | 207     |
| MOVIELENS     | 49.61  | 8.59  | 1.0     | 46.69  | 2.88 | 373     | 116.42          | 1.06  | 152     |
| ORL           | -1.51  | 4.39  | 1       | 2.84   | 1.92 | 386     | 3.65            | 4.29  | 58      |
| AL-GENES      | -0.32  | 0.29  | 15      | 0.01   | 2.39 | 161     | 0.07            | 19.43 | 61      |
| MANDRILL      | 3.25   | 2.3   | 1       | 6.53   | 2.37 | 404     | 6.14            | 3.16  | 43      |
| OZONE         | -39.92 | 0.74  | 2       | 0.03   | 3.23 | 211     | 0.16            | 16.76 | 24      |
| BRCA-GENES    | 11.39  | 5.17  | 0       | 14.19  | 2.18 | 371     | 4.97            | 39.44 | 29      |
| GOOGLE        | 11.22  | 4.4   | 4       | 18.78  | 2.55 | 145     | 22.63           | 7.16  | 17      |
| NPAS          | -71.29 | 15.86 | 0.2     | 8.55   | 3.93 | 246     | 17.57           | 19.52 | 23      |
| CAMERAMAN     | 1.69   | 3.64  | 0.3     | 5.67   | 3.44 | 102     | 14.44           | 24.83 | 18      |
| MOVIETRUST    | -2.37  | 4.05  | 0.3     | -20.79 | 4.23 | 209     | 22.49           | 10.49 | 10      |
| HEARTH        | -16.31 | 2.72  | 0       | 5.13   | 3.63 | 107     | 3.89            | 20.9  | 5       |
| IMAGENET      | 3.44   | 4.85  | 0.4     | 5.26   | 3.98 | 126     | 8.52            | 2.29  | 31      |

For our method, we also explore the trade-off between size and low-rankness by varying the value of  $\delta$ ; the results are presented in Appendix E.

## 8 Conclusion

Low-rank approximation finds applications in many data-analysis tasks. Typically, methods assume that the entire matrix exhibits low-rank structure, while in real-world data this is often true only for certain submatrices. In this work, we study the problem of finding submatrices that are provably close to a rank- $k$  approximation. We introduce a novel method that finds such submatrices, study the properties of the method, and, with a thorough experimental evaluation, we show that our method outperforms strong baselines.

There are several directions for future work. For instance, future work could study a more robust initialization strategy, develop more efficient and scalable alternative algorithms, and optimize the selection of the anchor rows and columns. It would also be valuable to investigate more the probabilistic aspects of our method. From a practical perspective, it would be interesting to explore further the benefits of our approach in different applications.

**Acknowledgments.** We thank the anonymous reviewers for their valuable comments, which helped us improve the paper.

Martino Ciaperoni is supported by the European Union through the ERC-2018-ADG GA 834756 (“XAI: Science and Technology for the Explanation of AI Decision-Making”) and the Partnership Extended PE00000013 (“FAIR: Future Artificial Intelligence Research”), Spoke 1: “Human-Centred AI”.

Aristides Gionis is supported by ERC Advanced Grant REBOUND (834862), EC H2020 RIA project SoBigData++ (871042), and the Wallenberg AI, Autonomous Systems and Software Program (WASP) funded by the Knut and Alice Wallenberg Foundation.

Heikki Mannila is supported by the Technology Industries of Finland Centennial Foundation.

## Appendix

### Appendix Contents

|  |    |
|--|----|
| – <b>Appendix A:</b> A Polynomial-time Algorithm to Find a Near-rank-1 Subset of Rows or Columns ..... | 22 |
| – <b>Appendix B:</b> Additional Analysis .....   | 23 |
| – <b>Appendix C:</b> Proofs .....  | 23 |
| – <b>Appendix D:</b> Details of Experimental Setup .....   | 33 |
| – <b>Appendix E:</b> Additional Experiments .....  | 37 |

### Appendix A A Polynomial-time Algorithm to Find a Near-rank-1 Subset of Rows or Columns

In this section, we give a simple algorithm that can be used to solve Problem 1 in polynomial time. The algorithm follows easily from the following result.

**Lemma 1.** *Consider two vectors  $\mathbf{x} \in \mathbb{R}^m$  and  $\mathbf{y} \in \mathbb{R}^m$  and let  $\boldsymbol{\epsilon} = \mathbf{y} - \text{Proj}_{\mathbf{x}} \mathbf{y}$ . We have:*

$$\|\boldsymbol{\epsilon}\|_2 = \|\mathbf{y}\|_2 \sin(\theta).$$

To solve Problem 1 optimally in polynomial time, i.e., to find a low-rank subset of rows for a fixed set of columns  $\mathcal{C}$ , we simply normalize the rows of  $\mathbf{D}$  to unit norm, and then compute the matrix  $\mathbf{S}_{\mathcal{C}}$  of pairwise sines, defined by:

$$\mathbf{S}_{\mathcal{C}} = \sqrt{1 - (\mathbf{D}\mathbf{D}^T)^2}.$$

The entry of indices  $i$  and  $j$  of  $\mathbf{S}_{\mathcal{C}}$  indicates the  $L_2$  norm of the error vector associated with the orthogonal projection of  $\mathbf{D}_{j,:}$  onto  $\mathbf{D}_{i,:}$ . Therefore, to find the largest possible set of rows, we perform a linear scan over the rows of  $\mathbf{S}_{\mathcal{C}}$  and for each row we pick the largest possible subset such that all elements satisfy the input error requirements. The solution to Problem 1 is given by the largest subset found while scanning the rows.

The solution to the symmetric problem asking for the largest subset of columns for a fixed set of rows  $\mathcal{R}$  can be found by simply inverting the role of the rows and columns in the algorithm.

## Appendix B Additional Analysis

Theorem 1 provides approximation guarantees for the near-rank-1 submatrices found by SAMPLEANDEXPAND. In more detail, the approximation guarantees are obtained for an interpretable approximation where each row or column is collinear with a single row or column. The approximation given by the SVD of the submatrices output by SAMPLEANDEXPAND also incurs bounded error in terms of Frobenius and spectral norm, but not necessarily in terms of max norm.

For the approximation given by the SVD, it is of particular interest to study the singular values. More specifically, since the spectral norm of a matrix is also equal to its largest singular value, it is interesting to study the spectral norm of the matrix of differences  $\mathbf{E}_{\mathbf{X}, \hat{\mathbf{X}}}$  obtained by using the rank-1 SVD to approximate a submatrix discovered by SAMPLEANDEXPAND. The following result provides a bound on the spectral norm of such matrix of differences.

**Theorem 2.** *Let  $\mathbf{X} \in \mathbb{R}^{n' \times m'}$  be a near-rank-1 submatrix output by SAMPLEANDEXPAND, with anchor row  $\mathbf{x}^r$ , anchor column  $\mathbf{x}^c$  and tolerance  $\delta$ . The matrix  $\mathbf{E}_{\mathbf{X}, \hat{\mathbf{X}}} = \mathbf{X} - \hat{\mathbf{X}}$  where  $\hat{\mathbf{X}}$  is the rank-1 approximation of  $\mathbf{X}$  given by SVD satisfies:*

$$\begin{aligned} \left\| \mathbf{E}_{\mathbf{X}, \hat{\mathbf{X}}} \right\|_2 \leq \min \left\{ \sqrt{\gamma \left( \frac{n' - 1}{n'} \right) - (n' - 1) \sqrt{1 - 8 \max_i \|\mathbf{X}_{i,:}\|_2^2 \delta^2 \omega_r (1 - \delta^2 \omega_r)}}, \right. \\ \left. \sqrt{\gamma \left( \frac{m' - 1}{m'} \right) - (m' - 1) \sqrt{1 - 8 \max_j \|\mathbf{X}_{:,j}\|_2^2 \delta^2 \omega_c (1 - \delta^2 \omega_c)}} \right\}, \end{aligned} \quad (6)$$

where  $\gamma = \|\mathbf{X}\|_F^2$ ,  $\omega_r = \frac{\sum_{i < j} x_i^{r^2} x_j^{r^2}}{\|\mathbf{x}^r\|_2^2 \min_i \|\mathbf{X}_{i,:}\|_2^2}$  and  $\omega_c = \frac{\sum_{i < j} x_i^{c^2} x_j^{c^2}}{\|\mathbf{x}^c\|_2^2 \min_j \|\mathbf{X}_{:,j}\|_2^2}$ .

Although the bound given in Theorem 2 is rather intricate, it could be considerably simplified by normalizing data, and its interpretation is similar to that of the bounds presented in Theorem 1. Like Theorem 1, Theorem 2 bounds the approximation error (in this case, in terms of spectral norm) based on the tolerance parameter  $\delta$ .

## Appendix C Proofs

### Appendix C.1 Proof of Lemma 1

Given two vectors  $\mathbf{y} \in \mathbb{R}^m$  and  $\mathbf{x} \in \mathbb{R}^m$ , the orthogonal projection of  $\mathbf{y}$  onto  $\mathbf{x}$  captures the component of  $\mathbf{y}$  that lies in the direction of  $\mathbf{x}$ . To prove Lemma 1, we need to show that the  $L_2$  norm of the difference between  $\mathbf{y}$  and its projection onto  $\mathbf{x}$  is equal to the  $L_2$  norm of  $\mathbf{y}$  multiplied by the sine of the angle  $\theta$  between  $\mathbf{y}$  and  $\mathbf{x}$ .

Recall that the projection of the vector  $\mathbf{y}$  onto the vector  $\mathbf{x}$  is given by:

$$\text{Proj}_{\mathbf{x}} \mathbf{y} = \frac{\mathbf{y}^T \mathbf{x}}{\mathbf{x}^T \mathbf{x}} \mathbf{x} = \frac{\mathbf{y}^T \mathbf{x}}{\|\mathbf{x}\|_2^2} \mathbf{x}.$$

The projection error  $\epsilon$  associated with  $\text{Proj}_{\mathbf{x}} \mathbf{y}$  is the vector given by the difference between  $\mathbf{y}$  and its projection onto  $\mathbf{x}$ , i.e.,

$$\epsilon = \mathbf{y} - \text{Proj}_{\mathbf{x}} \mathbf{y} = \mathbf{y} - \frac{\mathbf{y}^T \mathbf{x}}{\mathbf{x}^T \mathbf{x}} \mathbf{x}.$$

The  $L_2$  norm of the projection error  $\|\epsilon\|_2$  is thus  $\|\epsilon\|_2 = \left\| \mathbf{y} - \frac{\mathbf{y}^T \mathbf{x}}{\mathbf{x}^T \mathbf{x}} \mathbf{x} \right\|_2$ . By definition, the dot product  $\mathbf{y}^T \mathbf{x}$  can be expressed in terms of the  $L_2$  norm of  $\mathbf{y}$ , the  $L_2$  norm of  $\mathbf{x}$ , and the cosine of the angle  $\theta$  between  $\mathbf{y}$  and  $\mathbf{x}$  as follows:

$$\mathbf{y}^T \mathbf{x} = \|\mathbf{y}\|_2 \|\mathbf{x}\|_2 \cos(\theta).$$

Using this equality, we can rewrite the definition of the the projection error  $\epsilon$  as:

$$\epsilon = \mathbf{y} - \frac{\|\mathbf{y}\|_2 \|\mathbf{x}\|_2 \cos(\theta)}{\|\mathbf{x}\|_2^2} \mathbf{x} = \mathbf{y} - \frac{\|\mathbf{y}\|_2 \cos(\theta)}{\|\mathbf{x}\|_2} \mathbf{x}.$$

Further, the squared  $L_2$  norm of  $\epsilon$  becomes  $\left\| \mathbf{y} - \frac{\|\mathbf{y}\|_2 \cos(\theta)}{\|\mathbf{x}\|_2} \mathbf{x} \right\|_2^2$ . Since the projection error is orthogonal to the projection [29], the Pythagorean theorem yields:

$$\|\mathbf{y}\|_2^2 = \|\text{Proj}_{\mathbf{x}} \mathbf{y}\|_2^2 + \|\epsilon\|_2^2. \quad (7)$$

Because the  $L_2$  norm is equivariant under scalar multiplication, the  $L_2$  norm of the projection  $\|\text{Proj}_{\mathbf{x}} \mathbf{y}\|_2$  is:

$$\|\text{Proj}_{\mathbf{x}} \mathbf{y}\|_2 = \frac{\|\mathbf{y}\|_2 \|\mathbf{x}\|_2 \cos(\theta)}{\|\mathbf{x}\|_2} = \|\mathbf{y}\|_2 \cos(\theta).$$

Therefore, using Equation 7, the squared  $L_2$  norm of the projection error can be written as:

$$\|\epsilon\|_2^2 = \|\mathbf{y}\|_2^2 - \|\mathbf{y}\|_2^2 \cos^2(\theta) = \|\mathbf{y}\|_2^2 (1 - \cos^2(\theta)) = \|\mathbf{y}\|_2^2 \sin^2(\theta),$$

where we have employed the trigonometric identity  $1 - \cos^2(\theta) = \sin^2(\theta)$ . Finally, upon taking the square root of both sides, we get:

$$\|\epsilon\|_2 = \|\mathbf{y}\|_2 \sin(\theta).$$

Thus, we have shown that, as claimed, given the orthogonal projection of  $\mathbf{y}$  onto  $\mathbf{x}$ , the  $L_2$  norm of the projection error is equal to the  $L_2$  norm of  $\mathbf{y}$  multiplied by the sine of the angle  $\theta$  between  $\mathbf{y}$  and  $\mathbf{x}$ .

## Appendix C.2 Proof of Theorem 1

Before proceeding with the proof of Theorem 1, it is useful to prove the following lemma, which refers to the initialization phase only.

**Lemma 2.** Consider a  $2 \times 2$ -submatrix  $\mathbf{P}$  and let  $\mathbf{E}_\mathbf{P} = \mathbf{P} - \hat{\mathbf{P}}$ , where  $\hat{\mathbf{P}}$  is a rank-1 approximation of  $\mathbf{P}$ . If, as for the submatrices expanded by SAMPLEANDEXPAND,  $|\det(\mathbf{P})| \leq \delta_{init}$ ,  $\mathbf{P}$  admits rank-1 approximations  $\hat{\mathbf{P}}$  such that:

$$\|\mathbf{E}_\mathbf{P}\|_{\max} \leq \frac{\delta_{init} \max_{i,j} |\mathbf{D}_{i,j}|}{2 \min_{i,j} \mathbf{D}_{i,j}^2} \quad (8)$$

and

$$\|\mathbf{E}_\mathbf{P}\|_2 \leq \|\mathbf{E}_\mathbf{P}\|_F \leq \frac{\delta_{init}}{\gamma_{\max}}, \quad (9)$$

where  $\gamma_{\max}$  denotes the maximum  $L_2$  norm of a row or column of  $\mathbf{P}$ .

Lemma 2 is interesting not only because it provides a useful criterion to set the value of  $\delta_{init}$ , but it also formalizes the determinant-based notion of closeness to rank 1 for  $2 \times 2$  submatrices on which SAMPLEANDEXPAND builds. This notion is particularly simple; it only requires few basic operations, two products, a difference and possibly a change of sign, while knowledge of the (two) singular values is not required. Moreover, Lemma 2 is helpful for understanding the main result presented in Section 6, and its proof, given later in this section.

*Proof.* Consider a  $2 \times 2$  submatrix:

$$\mathbf{P} = \begin{pmatrix} x_1 & x_2 \\ y_1 & y_2 \end{pmatrix}.$$

We will start by proving the bound on the max norm of the  $2 \times 2$  matrix  $\mathbf{E}_\mathbf{P}$ , then we prove the bound on the Frobenius and spectral norms.

**Bound on the max norm.** In what follows, we let  $\mathbf{x} = (x_1, x_2)$  and  $\mathbf{y} = (y_1, y_2)$ . If  $\mathbf{P}$  has exactly rank 1, we have  $x_1y_2 = x_2y_1$  which is equivalent to  $\mathbf{x} = \alpha\mathbf{y}$  for some  $\alpha$ . In simple words,  $\mathbf{x}$  and  $\mathbf{y}$  are proportional. In the realistic case of data corrupted by noise, we are interested in near-rank-1  $2 \times 2$  submatrices, which are such that  $|x_1y_2 - x_2y_1| \leq \delta_{init}$  for some small  $\delta_{init}$ . If we approximate the rows of the matrix  $\mathbf{P}$  as  $\mathbf{x}$  and  $\alpha\mathbf{x}$  to obtain a rank-1 submatrix  $\hat{\mathbf{P}}$ , the only source of error is the approximation of  $\mathbf{y}$  as  $\alpha\mathbf{x}$ . Thus, define  $\epsilon_1 = y_1 - \alpha x_1$  and similarly  $\epsilon_2 = y_2 - \alpha x_2$ . The vector  $\boldsymbol{\epsilon} = (\epsilon_1, \epsilon_2)$  is referred to as error vector.

We can take  $\alpha$  to be the scalar that defines the orthogonal projection of  $\mathbf{y}$  onto  $\mathbf{x}$ . It is known that, for any orthogonal projection of a vector  $\mathbf{y}$  onto another  $\mathbf{x}$ , the vector  $\boldsymbol{\epsilon} = (\epsilon_1, \epsilon_2)$ , which we henceforth simply refer to as error vector, is orthogonal to  $\mathbf{x}$ . Therefore:

$$\boldsymbol{\epsilon}^T \mathbf{x} = \epsilon_1 x_1 + \epsilon_2 x_2 = 0,$$

from which we derive:

$$\epsilon_2 = -\frac{x_1}{x_2} \epsilon_1.$$

Furthermore, the condition we impose on the determinant means that:

$$|x_1y_2 - x_2y_1| \leq \delta_{init}.$$

Substituting the expression of  $\mathbf{y}$  as a linear function of  $\mathbf{x}$ , we obtain:

$$|x_1(\alpha x_2 + \epsilon_2) - x_2(\alpha x_1 + \epsilon_1)| \leq \delta_{init},$$

from which:

$$|x_1\epsilon_2 - x_2\epsilon_1| \leq \delta_{init}.$$

Substituting  $\epsilon_2 = -\frac{x_1}{x_2}\epsilon_1$  and collecting  $\epsilon_1$ , one gets:

$$\left| -\epsilon_1 \left( \frac{x_1^2}{x_2} + x_2 \right) \right| = \left| \epsilon_1 \left( \frac{x_1^2 + x_2^2}{x_2} \right) \right| \leq \delta_{init}.$$

Therefore, we conclude:

$$|\epsilon_1| \leq \frac{\delta_{init}|x_2|}{x_1^2 + x_2^2}.$$

As  $|\epsilon_1| = \frac{|x_2|}{|x_1|}|\epsilon_2|$ , we also have:

$$|\epsilon_2| \leq \frac{\delta_{init}|x_1|}{x_1^2 + x_2^2}.$$

Equation 8 follows by observing that we have no made any assumptions on  $x_1, x_2, y_1$  and  $y_2$ , and every entry must thus be bounded by  $\frac{\delta_{init} \max_{i,j} |\mathbf{D}_{i,j}|}{2 \min_{i,j} \mathbf{D}_{i,j}^2}$ .

**Bounds on the Frobenius and spectral norms.** To prove the bound on the Frobenius norm given in Equation 9, we again show that the bound holds for the rank-1 approximation  $\hat{\mathbf{P}}$  obtained by stacking the rows  $\mathbf{x} = (x_1, x_2)$  and  $\mathbf{y} = \alpha\mathbf{x}$ , where  $\alpha$  is the orthogonal-projection scalar, i.e.,  $\alpha = \frac{\mathbf{x}^T \mathbf{y}}{\|\mathbf{x}\|_2^2}$ . Because  $\mathbf{x}$  can be approximated with  $\mathbf{x}$  itself, the  $L_2$  norm of the projection error equals the Frobenius norm of the difference between  $\mathbf{P}$  and its rank-1 estimate  $\hat{\mathbf{P}}$ , i.e.,  $\|\epsilon\|_2 = \|\mathbf{P} - \hat{\mathbf{P}}\|_F = \|\mathbf{E}_\mathbf{P}\|_F$ .

Let  $\theta$  be the angle between the two vectors  $\mathbf{x}$  and  $\mathbf{y}$ . As stated in Lemma 1, we have that  $\|\epsilon\|_2 = \|\mathbf{y}\|_2 \sin(\theta)$ .

Next, we show that we additionally have the identity:

$$|x_1y_2 - x_2y_1| = \|\mathbf{x}\|_2 \|\mathbf{y}\|_2 \sin(\theta). \quad (10)$$

The  $L_2$  norms of  $\mathbf{x}$  and  $\mathbf{y}$  are:

$$\|\mathbf{x}\|_2 = \sqrt{x_1^2 + x_2^2} \text{ and } \|\mathbf{y}\|_2 = \sqrt{y_1^2 + y_2^2},$$

and the cosine of the angle  $\theta$  between the vectors  $\mathbf{x}$  and  $\mathbf{y}$  is given by:

$$\cos(\theta) = \frac{x_1y_1 + x_2y_2}{\|\mathbf{x}\|_2 \|\mathbf{y}\|_2}.$$

Using the identity  $\sin^2(\theta) + \cos^2(\theta) = 1$ , we get:

$$\sin^2(\theta) = 1 - \cos^2(\theta) = 1 - \left( \frac{x_1y_1 + x_2y_2}{\|\mathbf{x}\|_2 \|\mathbf{y}\|_2} \right)^2,$$

that is:

$$\sin^2(\theta) = \frac{(x_1^2 + x_2^2)(y_1^2 + y_2^2) - (x_1 y_1 + x_2 y_2)^2}{(x_1^2 + x_2^2)(y_1^2 + y_2^2)}.$$

Expanding and simplifying, one obtains:

$$\sin^2(\theta) = \frac{(x_1 y_2 - x_2 y_1)^2}{(x_1^2 + x_2^2)(y_1^2 + y_2^2)},$$

from which:

$$\sin^2(\theta) \|\mathbf{x}\|_2^2 \|\mathbf{y}\|_2^2 = (x_1 y_2 - x_2 y_1)^2,$$

and thus Equation 10 follows by taking the square root of both sides. As  $|x_1 y_2 - x_2 y_1| = \|\mathbf{x}\|_2 \|\mathbf{y}\|_2 \sin(\theta)$ , the condition  $|\det(\mathbf{P})| = |x_1 y_2 - x_2 y_1| \leq \delta_{init}$  implies:

$$\|\mathbf{x}\|_2 \|\mathbf{y}\|_2 \sin(\theta) \leq \delta_{init},$$

which holds if and only if:

$$\sin(\theta) \leq \frac{\delta_{init}}{\|\mathbf{x}\|_2 \|\mathbf{y}\|_2}.$$

Further, since  $\|\boldsymbol{\epsilon}\|_2 = \|\mathbf{y}\|_2 \sin(\theta)$ , we conclude:

$$\|\boldsymbol{\epsilon}\|_2 = \|\mathbf{E}_{\mathbf{P}}\|_F \leq \frac{\delta_{init}}{\|\mathbf{x}\|_2}.$$

We can swap the roles of  $\mathbf{x}$  and  $\mathbf{y}$  without changing the absolute value of the determinant, which leads to:

$$\|\boldsymbol{\epsilon}\|_2 = \|\mathbf{E}_{\mathbf{P}}\|_F \leq \frac{\delta_{init}}{\|\mathbf{y}\|_2}. \quad (11)$$

Similarly, swapping the columns does not change the absolute value of the determinant, which concludes the proof of the bound on the Frobenius norm. Finally, the spectral norm is always upper bounded by the Frobenius norm, and hence the lemma follows.

We are now in a position to prove Theorem 1, which describes the approximation-error guarantees associated with Algorithm 3 in terms of max, Frobenius and spectral norm. To prove the theorem, we extend the proof of Lemma 2 from the initialization to the expansion phase.

*Proof.* Like for the proof of Lemma 2, we prove bounds separately for the max norm and Frobenius and spectral norms. For simplicity, we present the proof for the row-wise ratios, and we denote by  $\mathbf{x}$  the anchor row, while  $\mathbf{y}$  denotes any other row of  $\mathbf{X}$ . The proofs for the column-wise ratios are always symmetric.

**Bound on the max norm.** The proof of the bound on the max norm (Equation 4) is straightforward, as it is a simple extension of the proof of the bound on the max norm given in Lemma 2 for the case of  $2 \times 2$  submatrices.

Given the anchor row  $\mathbf{x}^r$ , for every pair of entries  $(y_1, y_2)$  of another row  $\mathbf{y}$ , we consider the approximations  $y_1 = \alpha x_1^r$  and  $y_2 = \alpha x_2^r$  where  $\alpha$  is the orthogonal-projection scalar for the projection of  $\mathbf{y}$  onto  $\mathbf{x}^r$ .

The well-developed theory of orthogonal projections guarantees that the error vector  $\boldsymbol{\epsilon} = (\epsilon_1, \epsilon_2)$  is orthogonal to  $\mathbf{x}^r$  [29]. Therefore, we have:

$$\epsilon_1 x_1^r + \epsilon_2 x_2^r = 0,$$

i.e.,

$$\epsilon_2 = -\frac{x_1^r}{x_2^r} \epsilon_1.$$

The condition SAMPLEANDEXPAND imposes on the ratio matrices implies that:

$$\left| \frac{y_1}{x_1^r} - \frac{y_2}{x_2^r} \right| = \left| \frac{y_1 x_2^r - x_1^r y_2}{x_1^r x_2^r} \right| = \frac{|y_1 x_2^r - x_1^r y_2|}{|x_1^r| |x_2^r|} \leq \delta.$$

Substituting the expression of  $\mathbf{y}$  as a linear function of  $\mathbf{x}$ :

$$\frac{|(\alpha x_1^r + \epsilon_1) x_2^r - x_1^r (\alpha x_2^r + \epsilon_2)|}{|x_1^r| |x_2^r|} \leq \delta.$$

Simplifying:

$$\frac{|\epsilon_1 x_2^r - \epsilon_2 x_1^r|}{|x_1^r| |x_2^r|} \leq \delta \iff |\epsilon_1 x_2^r - \epsilon_2 x_1^r| \leq \delta |x_1^r| |x_2^r|.$$

Substituting  $\epsilon_2 = -\frac{x_1^r}{x_2^r} \epsilon_1$  and collecting  $\epsilon_1$ , one gets:

$$\left| \epsilon_1 \left( \frac{x_2^{r2} + x_1^{r2}}{x_2^r} \right) \right| \leq \delta |x_1^r| |x_2^r|,$$

from which we conclude:

$$|\epsilon_1| \leq \frac{\delta |x_1^r| |x_2^r|^2}{x_1^{r2} + x_2^{r2}}.$$

As  $|\epsilon_1| = \frac{|x_2^r|}{|x_1^r|} |\epsilon_2|$ , we also have:

$$|\epsilon_2| \leq \frac{\delta x_1^{r2} |x_2^r|}{x_1^{r2} + x_2^{r2}}.$$

We have no made any assumptions on  $x_1^r, x_2^r, y_1$  and  $y_2$ . Therefore, the bound:

$$\frac{\delta \max_i |x_i^r|^3}{2 \min_i x_i^{r2}}$$

necessarily hold for any entry in  $\mathbf{D}$ . Furthermore, a symmetric bound can be obtained by considering the column-wise ratios instead of the row-wise ones, and then Equation 4 follows.

**Bounds on the Frobenius and spectral norms.** To prove the theorem, we extend the proof of Equation 9 in Lemma 2 to the general case of  $n' \times m'$  submatrices. First notice that, given the orthogonal projection of a row  $\mathbf{y}$  onto  $\mathbf{x}^r$ , as in the case of Lemma 1, which does not make any assumption on the dimensions of the vectors under consideration, for the norm of the (now  $m'$ -dimensional) error vector, it holds that  $\|\boldsymbol{\epsilon}\|_2^2 = \|\mathbf{y}\|_2^2 \sin^2(\theta)$ .

In the expansion stage, we seek submatrices such that the  $2 \times 2$ -determinants within it are near zero. Instead of computing determinants, however, we compute ratios, which is more convenient. As already pointed out, the ratios that are computed in the expansion phase of our method are directly related to the determinants of the  $2 \times 2$ -submatrices. In particular, considering again row  $\mathbf{x}^r$  as the anchor row we divide by and another row  $\mathbf{y}$ , we require the following inequality on the ratios:

$$\left| \frac{y_i}{x_i^r} - \frac{y_j}{x_j^r} \right| \leq \delta \quad \text{for all } i \text{ and } j,$$

which implies:

$$|y_i x_j^r - y_j x_i^r| \leq |x_i^r| |x_j^r| \delta \quad \text{for all } i \text{ and } j.$$

Thus, the bound on the absolute difference of ratios guarantees that the associated  $2 \times 2$ -submatrix determinant is bounded by  $\delta$ , rescaled by the absolute values of the entries  $x_i^r$  and  $x_j^r$  of the anchor row.

Keeping in mind the relationship between ratios and  $2 \times 2$  determinants, we continue the proof by finding a bound on the the norm of the error vector  $\|\boldsymbol{\epsilon}\|_2^2 = \|\mathbf{y}\|_2^2 \sin^2(\theta)$  obtained by projecting  $\mathbf{y}$  onto  $\mathbf{x}^r$ . In particular, to find a bound for  $\|\boldsymbol{\epsilon}\|_2^2$ , we need to bound  $\sin^2(\theta)$ . First, notice that:

$$\sin^2(\theta) = 1 - \cos^2(\theta) = 1 - \frac{(\mathbf{x}^r)^T \mathbf{y})^2}{\|\mathbf{x}^r\|_2^2 \|\mathbf{y}\|_2^2} = \frac{\|\mathbf{x}^r\|_2^2 \|\mathbf{y}\|_2^2 - (\mathbf{x}^r)^T \mathbf{y})^2}{\|\mathbf{x}^r\|_2^2 \|\mathbf{y}\|_2^2}.$$

Let us focus on the numerator,  $\|\mathbf{x}^r\|_2^2 \|\mathbf{y}\|_2^2 - (\mathbf{x}^r)^T \mathbf{y})^2$ . For simplicity, in what follows, we use the notation  $\sum_{i \neq j}$  to denote the sum over pairs  $(i, j)$  from 1 to  $m'$  such that  $i \neq j$ , and, similarly, the notation  $\sum_{i < j}$  to indicate the sum over pairs  $(i, j)$  from 1 to  $m'$  such that  $i$  is lower than  $j$ . Expanding the product of the squared  $L_2$  norms, one obtains:

$$\|\mathbf{x}^r\|_2^2 \|\mathbf{y}\|_2^2 = \left( \sum_{i=1}^{m'} x_i^r \right)^2 \left( \sum_{j=1}^{m'} y_j^2 \right) = \sum_{i=1}^{m'} x_i^r x_i^r y_i^2 + \sum_{i \neq j} x_i^r x_j^r y_i^2 y_j^2.$$

Similarly, expanding the squared dot product, we get:

$$(\mathbf{x}^r)^T \mathbf{y})^2 = \sum_{i=1}^{m'} x_i^r x_i^r y_i^2 + 2 \sum_{i < j} x_i^r y_i x_j^r y_j.$$

Thus:

$$\|\mathbf{x}^r\|_2^2 \|\mathbf{y}\|_2^2 - (\mathbf{x}^{rT} \mathbf{y})^2 = \sum_{i=1}^{m'} x_i^{r2} y_i^2 + \sum_{i \neq j} x_i^{r2} y_j^2 - \left( \sum_{i=1}^{m'} x_i^{r2} y_i^2 + 2 \sum_{i < j} x_i^r y_i x_j^r y_j \right).$$

Canceling out the terms  $\sum_{i=1}^{m'} x_i^{r2} y_i^2$ , we are left with:

$$\sum_{i \neq j} x_i^{r2} y_j^2 - 2 \sum_{i < j} x_i^r y_i x_j^r y_j,$$

By symmetry, the term  $\sum_{i \neq j} x_i^{r2} y_j^2$  can be rewritten as  $\sum_{i < j} (x_i^{r2} y_j^2 + x_j^{r2} y_i^2)$ , and hence:

$$\begin{aligned} \sum_{i \neq j} x_i^{r2} y_j^2 - 2 \sum_{i < j} x_i^r y_i x_j^r y_j &= \\ \sum_{i < j} (x_i^{r2} y_j^2 + x_j^{r2} y_i^2) - 2 \sum_{i < j} x_i^r y_i x_j^r y_j &= \sum_{i < j} (x_i^{r2} y_j^2 + x_j^{r2} y_i^2 - 2 x_i^r y_i x_j^r y_j). \end{aligned}$$

The expression above corresponds to a sum of squared differences. Specifically, it is equivalent to:

$$\sum_{i < j} (y_i x_j^r - y_j x_i^r)^2.$$

Thus, we have shown that:

$$\|\mathbf{x}^r\|_2^2 \|\mathbf{y}\|_2^2 - (\mathbf{x}^{rT} \mathbf{y})^2 = \sum_{i < j} (y_i x_j^r - y_j x_i^r)^2.$$

As explained above, the condition we impose on the ratios leads to  $|y_i x_j^r - y_j x_i^r| \leq |x_i^r| |x_j^r| \delta$ , or, equivalently  $(y_i x_j^r - y_j x_i^r)^2 \leq x_i^{r2} x_j^{r2} \delta^2$ . Therefore:

$$\sin^2(\theta) = \frac{\|\mathbf{x}^r\|_2^2 \|\mathbf{y}\|_2^2 - (\mathbf{x}^{rT} \mathbf{y})^2}{\|\mathbf{x}^r\|_2^2 \|\mathbf{y}\|_2^2} = \frac{\sum_{i < j} (x_i^r y_j - x_j^r y_i)^2}{\|\mathbf{x}^r\|_2^2 \|\mathbf{y}\|_2^2} \leq \frac{\delta^2 \sum_{i < j} x_i^{r2} x_j^{r2}}{\|\mathbf{x}^r\|_2^2 \|\mathbf{y}\|_2^2}.$$

Finally, recalling that  $\|\boldsymbol{\epsilon}\|_2^2 = \|\mathbf{y}\|_2^2 \sin^2(\theta)$ , we have:

$$\|\boldsymbol{\epsilon}\|_2^2 \leq \frac{\delta^2 \sum_{i < j} x_i^{r2} x_j^{r2}}{\|\mathbf{x}^r\|_2^2}. \quad (12)$$

Equation 12 applies to every non-anchor row  $\mathbf{y}$  of  $\mathbf{X}$ . As usual, the same derivations also hold for the columns of  $\mathbf{X}$ . Hence, the bound on the Frobenius stated in the theorem follows, and the spectral norm is always bounded by the Frobenius norm. This concludes the proof of the theorem.

### Appendix C.3 Proof of Theorem 2

To conclude this section, we present the proof of Theorem 2 which bounds the low-rank-approximation error incurred by the rank-1 SVD for the submatrices detected by SAMPLEANDEXPAND.

*Proof.* To prove the bound on the spectral norm of the matrix of differences  $\mathbf{E}_{\mathbf{X}, \hat{\mathbf{X}}}$  obtained by approximating a near-rank-1 submatrix discovered by SAMPLE-ANDEXPAND through its rank-1 SVD, we again consider the rows of  $\mathbf{X}$  and we reuse the bound on the sine of the angle  $\theta$  between a row  $\mathbf{y}$  and the anchor row  $\mathbf{x}^r$  obtained in the proof of Theorem 1. Specifically, while proving the bound on the Frobenius and spectral norms in Equation 5, we have shown that:

$$\sin^2(\theta) \leq \frac{\|\mathbf{x}^r\|_2^2 \|\mathbf{y}\|_2^2 - (\mathbf{x}^r \mathbf{y})^2}{\|\mathbf{x}^r\|_2^2 \|\mathbf{y}\|_2^2} = \frac{\sum_{i < j} (x_i^r y_j - x_j^r y_i)^2}{\|\mathbf{x}^r\|_2^2 \|\mathbf{y}\|_2^2} \leq \frac{\delta^2 \sum_{i < j} x_i^r x_j^r}{\|\mathbf{x}^r\|_2^2 \|\mathbf{y}\|_2^2}.$$

For ease of notation, we let  $\mathbf{y}_{min}$  denote the non-anchor row  $\mathbf{y}$  of minimum squared  $L_2$  norm in  $\mathbf{D}$  and  $\tau = \frac{\delta^2 \sum_{i < j} x_i^r x_j^r}{\|\mathbf{x}^r\|_2^2 \|\mathbf{y}_{min}\|_2^2}$ , which corresponds to the largest possible bound on  $\sin^2(\theta)$  across all rows of  $\mathbf{X}$ , and will be useful later in the proof.

A widely-known result in linear algebra guarantees that the square of a singular value of  $\mathbf{X}$  is equal to the corresponding eigenvalue of the symmetric and positive semi-definite Gram matrix  $\mathbf{G} = \mathbf{X} \mathbf{X}^T \in \mathbb{R}^{n' \times n'}$  [29]. Consider the rank-1 approximation  $\hat{\mathbf{X}}$  of  $\mathbf{X}$  given by the SVD. Subtracting  $\hat{\mathbf{X}}$  from  $\mathbf{X}$  cancels out the leading (i.e., largest) singular value of  $\mathbf{X}$ . Thus, to prove an upper bound on the spectral norm of  $\mathbf{E}_{\mathbf{X}, \hat{\mathbf{X}}}$ , we prove an upper bound on the second largest singular value of  $\mathbf{X}$ , which is equivalent to the square root of the largest eigenvalue  $\lambda_{max}(\mathbf{G})$  of  $\mathbf{G}$ . To find an upper bound on the the second largest eigenvalue of  $\mathbf{G}$ , we start by deriving a lower bound on the largest eigenvalue. Such lower bound follows from the inequality  $\sin^2(\theta) \leq \tau$  which holds for all angles  $\theta$  between the anchor row  $\mathbf{x}^r$  and any other row  $\mathbf{y}$ . Intuitively, this inequality suggests that all the row vectors are aligned to the same vector  $\mathbf{x}$ . Thus, the angle between any two non-anchor rows cannot be arbitrarily large. More precisely, the angle between  $\mathbf{y}_i$  and  $\mathbf{y}_j$  can be at most equal to the sum of the angles between  $\mathbf{y}_i$  and  $\mathbf{x}^r$  and between  $\mathbf{y}_j$  and  $\mathbf{x}^r$ . In this case, we have:

$$\cos(\theta_{i,j}) = \cos(\theta_i) \cos(\theta_j) - \sin(\theta_i) \sin(\theta_j),$$

where  $\theta_i$  and  $\theta_j$  denote the angle between  $\mathbf{y}_i$  and  $\mathbf{x}^r$  and the angle between  $\mathbf{y}_j$  and  $\mathbf{x}^r$ , respectively, whose squared sines are bounded by  $\tau$ . Recalling that the squared cosine equals the complement to 1 of the squared sine, we obtain:

$$\cos(\theta_{i,j}) \geq (\sqrt{1 - \tau} \sqrt{1 - \tau}) - (\sqrt{\tau} \sqrt{\tau}),$$

i.e.,  $\cos(\theta_{i,j}) \geq 1 - 2\tau$ , which is equivalent to:

$$\sin^2(\theta_{i,j}) \leq 4\tau(1 - \tau).$$

We have obtained an upper bound on the squared sine of the angle between any pair of non-anchor rows in  $\mathbf{X}$ , which translates into a lower bound on the inner product. In particular, we have that:

$$\sin^2(\theta_{i,j}) = 1 - \cos^2(\theta_{i,j}) = 1 - \frac{(\mathbf{y}_i^T \mathbf{y}_j)^2}{\|\mathbf{y}_i\|_2^2 \|\mathbf{y}_j\|_2^2} \leq 4\tau(1 - \tau),$$

implying:

$$-(\mathbf{y}_i^T \mathbf{y}_j)^2 \leq 4\tau(1 - \tau) \|\mathbf{y}_i\|_2^2 \|\mathbf{y}_j\|_2^2 - 1,$$

and from which:

$$\mathbf{y}_i^T \mathbf{y}_j \geq \sqrt{1 - 4\tau(1 - \tau) \|\mathbf{y}_i\|_2^2 \|\mathbf{y}_j\|_2^2}.$$

A bound that holds for all possible pairs of rows  $\mathbf{y}_i$  and  $\mathbf{y}_j$  is thus:

$$\sqrt{1 - 8\tau(1 - \tau) \|\mathbf{y}_{max}\|^2},$$

where  $\mathbf{y}_{max}$  denotes the non-anchor row of maximum  $L_2$  norm.

Now that we have obtained a lower bound on the inner products between any pair of rows of  $\mathbf{X}$ , note that the inner products correspond precisely to the off-diagonal entries of  $\mathbf{G}$ , while the diagonal entries of  $\mathbf{G}$  are all of the form  $\mathbf{y}_i^T \mathbf{y}_i = \|\mathbf{y}_i\|_2^2$ . It is known that the largest eigenvalue of a matrix can be found by maximizing Rayleigh quotient [29], i.e., it satisfies:

$$\lambda_{\max}(\mathbf{G}) = \max_{\mathbf{v} \neq 0} \frac{\mathbf{v}^T \mathbf{G} \mathbf{v}}{\mathbf{v}^T \mathbf{v}}.$$

Choosing  $\mathbf{v} = (1, 1, \dots, 1)^T \in \mathbb{R}^{1 \times n'}$ , we get:

$$\mathbf{v}^T \mathbf{G} \mathbf{v} = \sum_{i,j} \mathbf{G}_{ij} \geq \|\mathbf{X}\|_F^2 + (n' - 1)n'\tau',$$

where  $\tau' = \sqrt{1 - 8\tau(1 - \tau) \|\mathbf{y}_{max}\|^2}$ . Since the denominator of Rayleigh quotient  $\mathbf{v}^T \mathbf{v}$  takes value  $n'$ , we obtain:

$$\lambda_{\max}(\mathbf{G}) \geq \frac{\|\mathbf{X}\|_F^2}{n'} + (n' - 1)\tau'.$$

Thus, for the largest singular value  $\sigma_1(\mathbf{X})$  of  $\mathbf{X}$ , we have that  $\sigma_1(\mathbf{X}) \geq \sqrt{\frac{\|\mathbf{X}\|_F^2}{n'} + (n' - 1)\tau'}$ . We also have the equality [29]:

$$\sum_{i=1}^n \lambda_i(\mathbf{G}) = \text{Tr}(\mathbf{G}) = \|\mathbf{X}\|_F^2.$$

Therefore, since  $\lambda_{\max}(\mathbf{G}) \geq \frac{\|\mathbf{X}\|_F^2}{n'} + (n' - 1)\tau'$ , and the eigenvalues after the first one cannot be larger than the first one, the remaining eigenvalues satisfy:

$$\sum_{i=2}^{n'} \lambda_i(\mathbf{G}) \leq \|\mathbf{X}\|_F^2 - \left( \frac{\|\mathbf{X}\|_F^2}{n'} + (n' - 1)\tau' \right) = \|\mathbf{X}\|_F^2 - \frac{\|\mathbf{X}\|_F^2}{n'} - (n' - 1)\tau'.$$

Hence, we get:

$$\lambda_2(\mathbf{G}) \leq \|\mathbf{X}\|_F^2 - \frac{\|\mathbf{X}\|_F^2}{n'} - (n' - 1)\tau'.$$

As a consequence, recalling the definition of  $\tau'$ , we can conclude:

$$\begin{aligned} \|\mathbf{E}_{\mathbf{X}, \hat{\mathbf{X}}}\|_2 &\leq \sigma_2(\mathbf{X}) \leq \\ \sqrt{\|\mathbf{X}\|_F^2 - \frac{\|\mathbf{X}\|_F^2}{n'} - (n' - 1)\sqrt{1 - 8 \max \|\mathbf{X}_{i,:}\|_2^2 \frac{\delta^2 \sum_{i < j} x_i^r x_j^r}{\|\mathbf{x}\|_2^2 \min_i \|\mathbf{X}_{i,:}\|_2^2} (1 - \frac{\delta^2 \sum_{i < j} x_i^r x_j^r}{\|\mathbf{x}\|_2^2 \min_i \|\mathbf{X}_{i,:}\|_2^2})}}}. \end{aligned}$$

As usual, the same derivations also apply to the columns of  $\mathbf{X}$ , which concludes the proof.

## Appendix D Details of Experimental Setup

**Datasets.** To generate synthetic data, we proceed as follows.

- First, we generate vectors  $\mathbf{x} \in \mathbb{R}^{n'}$  and  $\mathbf{y} \in \mathbb{R}^{m'}$  according to a given probability distribution  $\mathcal{P}$ .
- We then compute the rank-1 matrix  $\mathbf{X} = \mathbf{x}\mathbf{y}^T \in \mathbb{R}^{n' \times m'}$ , and we inject additive noise generated according to the probability distribution  $\mathcal{P}$ , rescaled by a factor  $\epsilon_{noise}$  and re-centered to have 0 mean. The larger the parameter  $\epsilon_{noise}$ , the higher the noise and the more  $\mathbf{X}$  deviates from a rank-1 matrix.
- We finally generate a larger matrix  $\mathbf{D} \in \mathbb{R}^{n \times m}$  by resampling uniformly at random the entries of the submatrix  $\mathbf{X}$  and planting the near-rank-1 submatrix in randomly-sampled row indices  $\mathcal{R}'$  and column indices  $\mathcal{C}'$ .

The above data-generating mechanism is designed to make the task of near-rank-1 submatrix recovery as challenging as possible. If the distribution of the entries in the near-rank-1 submatrix deviates significantly from the remaining entries (or background), then co-clustering algorithms may suffice to discover the submatrix. We consider different choices for the distribution  $\mathcal{P}$ , namely standard normal, uniform in  $[0, 1]$ , exponential of rate 1, Beta with parameters 2 and 3, Gamma with shape 2 and scale 1 and Poisson of rate 5.

We always consider synthetic matrices  $\mathbf{D} \in \mathbb{R}^{n \times m}$  with  $n = 250$  and  $m = 250$ , and the parameter  $\epsilon_{noise}$  is set to  $1^{-5}$ , unless stated otherwise.

In the experiments carried out to evaluate the performance of SAMPLEANDEXPAND against the baselines, we first plant near-rank-1 square submatrices of increasing size  $n' \times n'$  with  $n' \in \{25, 50, 75, 100, 125\}$ .

In addition to the synthetic data with a single planted near-rank-1 submatrix, we also consider the general setting that involves multiple planted near-rank-1 submatrices. More formally, we generate:

$$\mathbf{X} = \sum_{h=1}^{N_{patterns}} \mathbf{X}_h^*,$$

where:

$$\mathbf{X}_h^* = \begin{cases} \mathbf{X}_{h_{i,j}}, & \text{if } i \in \mathcal{R}_h \text{ and } j \in \mathcal{C}_h \\ 0, & \text{otherwise,} \end{cases}$$

and  $\mathbf{X}_h$  is generated as explained above and planted in row indices  $\mathcal{R}_h$  and column indices  $\mathcal{C}_h$ . In the experiments, we consider  $N_{patterns} \in \{1, 2, 3, 4, 5\}$ , and we sample  $n'$  and  $m'$  uniformly at random between 20 and 75. For the purposes of the experimental evaluation, it is assumed that each method is aware of the number of planted submatrices. Thus, each method (iteratively) discovers  $N_{patterns}$  submatrices. In particular, SAMPLEANDEXPAND follows the procedure sketched in Algorithm 2. A key point to highlight is that although all the generated matrices  $\mathbf{X}_h^*$  are close to rank 1, they can overlap with each other, yielding intersection submatrices that are close to a low-rank structure, but not necessarily close to rank 1. The overlap between different planted submatrices makes the task of discovering near-low-rank submatrices more challenging than in the case of a single planted near-rank-1 submatrix. In fact, in the absence of overlap between different planted submatrices, our method can simply iteratively discover each submatrix independently of the others.

As concerns real-world datasets, we consider 15 heterogeneous matrices coming from different domains. Summary characteristics and references are provided in Table 1 in Section 7.1. We choose data matrices from different domains that are common in the low-rank-approximation literature. In particular, we consider benchmark datasets for supervised-learning tasks (ISOLET, OZONE, HEARTH), image datasets (OLIVETTI, ORL, MANDRILL and CAMERAMAN), benchmark datasets for recommender systems (MOVIELENS, GOOGLE and MOVIETRUST), gene-expression data (AL-GENES and BRCA-GENES), neural-network weights (IMAGENET), and two miscellaneous datasets (HYPERSPECTRAL and NPAS).

**Metrics.** Here, we offer more details on the performance metrics adopted to assess the performance of SAMPLEANDEXPAND against the baselines, which are briefly discussed in Section 7.1.

When the ground truth is available, i.e., in synthetic data, we can assess the performance of a method in recovering the ground truth by the (balanced)  $F_1$  score, which is a widely used metric in binary classification and information-retrieval tasks. The  $F_1$  score corresponds to the harmonic mean of precision and recall. Formally, it is defined as  $F_1 = \frac{2 \cdot \text{TP}}{2 \cdot \text{TP} + \text{FP} + \text{FN}}$ , where TP, FP, FN are the true positives, false positives and false negatives, respectively. A method assigns a nonzero value to all the entries with indices in the discovered submatrices and zero to the remaining entries. The nonzero values, in particular, are given by the low-rank approximation of the discovered submatrices. A true positive occurs when a method assigns a nonzero value to an entry in a planted near-rank-1 submatrix. Similarly, a false positive occurs when the method assigns a nonzero value to an entry that is not part of a planted near-rank-1 submatrix. Finally, false negatives correspond to those entries for which a method predicts a zero value in one of the entries that are part of a planted near-rank-1 submatrix.

Given the ground truth, in addition to the  $F_1$  score, it is of primary importance to assess the estimate of a planted submatrix that is given by a method. For this

purpose, we compute the reconstruction error, which is given by:

$$\|\mathbf{E}_{\mathbf{X}, \hat{\mathbf{X}}}\|_F^2 = \|\mathbf{X} - \hat{\mathbf{X}}\|_F^2,$$

where  $\mathbf{X}$  is a ground-truth near-rank-1 submatrix and  $\hat{\mathbf{X}}$  its estimate. The choice of the squared Frobenius norm is standard, but any other norm could be considered instead. To ensure that the error is comparable across submatrices of varying sizes, we report the reconstruction error averaged over all entries of  $\mathbf{X}$ .

In real-world datasets no ground truth is available. In this case, there are two fundamental quantities that should be monitored; a measure of closeness to a low-rank matrix and a measure of size. The measure of closeness to a low-rank matrix is the crucial quantity. However, the size of the submatrices is also important. The two quantities are typically inversely related; it is always possible to obtain a perfectly rank-1 submatrix by reducing its size, and vice versa, it is always possible to obtain a submatrix as large as the input matrix by making it deviate more and more from a rank-1 submatrix. Thus, a method is preferred over another whenever it strikes a more desirable balance between closeness to rank 1 and size.

As regards closeness to a rank-1 matrix, we monitor the low-rankness score, introduced in Section 3. For a submatrix  $\mathbf{X} \in \mathbb{R}^{n' \times m'}$  with  $i$ -th singular value  $\sigma_i^2$ , the low-rankness score is defined as  $\ell r(\mathbf{X}) = \frac{\sigma_1(\mathbf{X})^2}{\sum_{i=1}^{\min(n', m')} \sigma_i(\mathbf{X})^2}$ . The low-rankness score has been adopted in previous work to monitor the performance in experiments with real-world datasets [7]. It mathematically equals the reciprocal of the popular stable-rank measure. The low-rankness scores ranges between 0 and 1. The closer the low-rankness score is to 1, the closer the submatrix is to the ideal scenario of rank exactly 1. It is important to consider the low-rankness of a submatrix in relation to the input matrix it is extracted from. A submatrix of size  $n' \times m'$  with a low-rankness score of 0.95 is extremely desirable if the low-rankness score of the input matrix is 0.3. However, the same submatrix is not as desirable when the low-rankness score of the input matrix is 0.9. Therefore, to facilitate the understanding of the results, in addition to the raw low-rankness scores of the top-5 output submatrices, we also report the average relative percentage increase in low-rankness with respect to the input matrix. The relative percentage increase in low-rankness is given by:

$$\frac{\ell r(\mathbf{X}) - \ell r(\mathbf{D})}{\ell r(\mathbf{D})} \cdot 100,$$

where  $\ell r(\mathbf{X})$  and  $\ell r(\mathbf{D})$  indicate the low-rankness score of an output submatrix  $\mathbf{X}$  and of the input matrix  $\mathbf{D}$ , respectively. An important point to highlight is that, while the rank of a submatrix can never exceed that of the larger matrix it is contained in, the low-rankness score of a submatrix can be smaller than that of the matrix it is contained in. Therefore, the relative percentage increase in low-rankness can be negative.

Finally, also for the size of an output submatrix, as for the low-rankness score, it is important to consider the size of the submatrix in relation to the size of the

input matrix. Therefore, in addition to the raw number  $|\mathbf{X}|$  of entries in the top-5 output submatrices, we report the percentage  $\frac{|\mathbf{X}|}{|\mathbf{D}|} \cdot 100$  of entries in the input matrix that are part of the output submatrix, averaged over the top-5 output submatrices.

**Parameters settings.** In this paragraph, we provide more details concerning the parameter settings for the methods considered in the experiments.

In Section 7.1, we discuss the values of the parameters  $\delta$  and  $\delta_{init}$  used in the experiments. In addition to  $\delta$  and  $\delta_{init}$ , the other important parameter to be given in input to SAMPLEANDEXPAND is the target rank  $k$ . If  $k = 1$ , SAMPLEANDEXPAND utilizes Algorithm 3 to discover near-rank-1 submatrices, otherwise it uses Algorithm 4 to discover near-rank- $k$  submatrices. In the experiments with synthetic data, when the number of planted patterns is 1, we consider  $k = 1$ , when it is between 2 and 4, we consider  $k = 1$  and  $k = 2$ , and finally when there are 5 patterns, we additionally consider  $k = 3$ . In all cases, however, the total number of initialization is  $N_{init} = 25$ . In the case of real-world data, we always consider  $k = 1$ .

Finally, the parameter  $\lambda$  in the objective function  $f$  controlling the relative weight of reconstruction error and size is held constant to its default value of 1.

As concerns the baselines, for sparse PCA, we set the sparsity-controlling parameter  $\alpha$  to 1. In the convex-optimization-based approach, we set the parameter  $\theta$  controlling the trade-off between nuclear and  $L_1$  norm to 10. SVP is a parameter-free method. Finally, RPSP samples  $10^5$   $2 \times 2$  and  $4 \times 4$  submatrices and  $10^4$   $8 \times 8$  and  $16 \times 16$  submatrices and the number of score matrices that are computed (and summed up) before finding the final solution is set to 30.

**Implementation details.** We conclude this section by providing details regarding the implementation of SAMPLEANDEXPAND and of the baseline approaches.

An important choice for the implementation of SAMPLEANDEXPAND is the approach leveraged to extract a maximum-edge biclique in the bipartite graph  $\mathcal{G}_{\mathbf{I}}$ . In all the experiments with synthetic data, we leverage the algorithm of Lyu et al. [22] for mining maximum-edge bicliques and we rely on an implementation in C of the algorithm available online.<sup>5</sup>

In the experiments with real-data, to eschew possible scalability issues, we heuristically extract dense submatrices from the indicator matrix  $\mathbf{I}$  via spectral biclustering [19], which, as discussed in Section 5, is the heuristic of choice to approximate maximum-edge bicliques. This algorithm is not guaranteed to return submatrices of  $\mathbf{I}$  consisting of all ones (i.e., bicliques). Subsequently, the guarantees reported in Theorem 1 may not hold when spectral biclustering is used. Despite the lack of theoretical guarantees, the implementation of SAMPLEANDEXPAND using spectral biclustering is effective in practice, as demonstrated by our experiments.

To approximate the discovered submatrices, we use the interpretable approximation in terms of the original rows or columns of the data if the target rank is 1 and the SVD otherwise.

---

<sup>5</sup> <https://github.com/wonghang/pymbc>

For spectral biclustering, we use the implementation available in the SCIKIT-LEARN PYTHON library.<sup>6</sup>

To handle sparse datasets, we also implement particular constraints that avoid returning trivial rank-1 submatrices consisting of all zeros.

As for the baselines, we implement SVP in PYTHON. For RPSP, we instead rely on the implementation provided by the authors.<sup>7</sup> For SPARSEPCA and for the convex-optimization approach (CVX), we use the SCIKIT-LEARN<sup>8</sup> and CVXPY<sup>9</sup> PYTHON libraries, respectively.

## Appendix E Additional Experiments

In this section, we present additional experimental results. First, we present preliminary experiments, and then we present additional results of experiments evaluating the performance of the method we introduce in both synthetic and real data.

**Preliminary experiments.** The goal of the preliminary experiments is to provide valuable insights into the synthetic data used in our experiments, and on the behavior of SAMPLEANDEXPAND in such data.

We first consider a full-rank  $250 \times 250$  matrix with all i.i.d. entries generated from a standard normal distribution and no planted near-rank-1 submatrix. For such matrix, in Figure 7, we show the distribution of the determinants of the initially-sampled  $2 \times 2$  matrices as well as the probability of hitting a near-rank-1  $2 \times 2$  submatrix with near-zero determinant as a function of the parameter  $\delta_{init}$  (with  $\delta_{init} \in \{10^{-8}, 10^{-7}, 10^{-6}, 10^{-5}, 10^{-4}\}$ ). Finally, we show the average reconstruction error  $\left\| \mathbf{E}_{\mathbf{x}, \hat{\mathbf{x}}} \right\|_F^2$  of the submatrices retrieved by SAMPLEANDEXPAND as a function of the proportion of entries of the input matrix they include. As Figure 7 suggests, although the input matrix is generated completely at random and with no planted near-rank-1 submatrix, it still contain many  $2 \times 2$  submatrices with near-zero determinant, and the probability of SAMPLEANDEXPAND hitting a near-rank-1  $2 \times 2$  submatrix in the initialization phase quickly grows as the initial tolerance parameter  $\delta_{init}$  is increased, confirming the intuition gained through the simple probabilistic analysis presented in Section 6. However, no large matrix with small reconstruction error is found at the expansion phase, since, unlike in real-world matrices, it is unlikely that large low-rank submatrices occur in matrices consisting solely of i.i.d. entries.

Figure 8 presents similar results as Figure 7, but for a synthetic  $250 \times 250$  matrix where a near-rank-1 submatrix is generated from a standard normal distribution and planted according to the procedure illustrated in Appendix D. In particular, for such matrix, the figure shows the distribution of the values in the planted

<sup>6</sup> <https://scikit-learn.org/stable/modules/generated/sklearn.cluster.SpectralBiclustering.html>

<sup>7</sup> <https://github.com/ptdang1001/RPSP>

<sup>8</sup> <https://scikit-learn.org/stable/modules/generated/sklearn.decomposition.SparsePCA.html>

<sup>9</sup> <https://www.cvxpy.org>

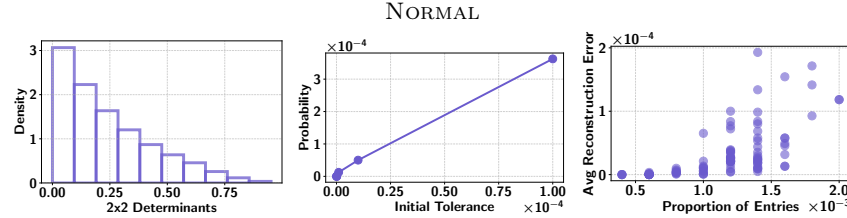


Fig. 7: Full-rank  $250 \times 250$  synthetic matrix with i.i.d entries from a standard normal distribution and without planted near-rank-1 submatrices. We show the distribution of  $2 \times 2$ -submatrix determinants (left), the probability of observing a  $2 \times 2$ -submatrix with determinant in absolute value lower than the initial tolerance threshold  $\delta_{init}$  as a function of  $\delta_{init}$  (center) and the (per-entry) average reconstruction error as a function of the proportion of entries in the submatrix for individual iterations of our method (right).

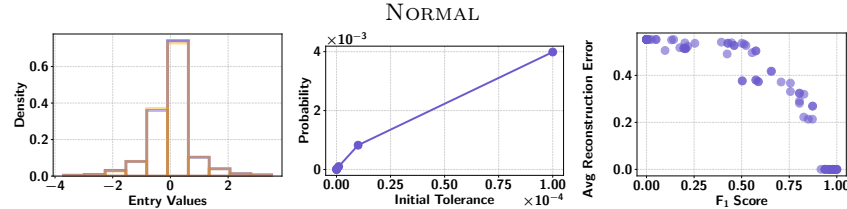


Fig. 8: Full-rank synthetic  $250 \times 250$  matrix generated from a standard normal distribution and with a  $25 \times 25$  planted near-rank-1 submatrix. We show the distribution of the values in the entire matrix and submatrix (left), the probability of observing a  $2 \times 2$ -submatrix with determinant in absolute value lower than the initial tolerance threshold  $\delta_{init}$  as a function  $\delta_{init}$  (center) and the (per-entry) average reconstruction error as a function of the  $F_1$  score for individual iterations of our method (right).

near-rank-1 submatrices and in the background, the probability that SAMPLE-ANDEXPAND samples a near-rank-1  $2 \times 2$  submatrix in the initialization phase as a function of the parameter  $\delta_{init}$  (with  $\delta_{init} \in \{10^{-8}, 10^{-7}, 10^{-6}, 10^{-5}, 10^{-4}\}$ ) and the average reconstruction error as a function of the  $F_1$  score for the submatrices output by our method in different iterations. The figure demonstrates that the planted near-rank-1 submatrices are drawn from the same distribution as the background, reflecting a scenario where standard co-clustering algorithms are generally not able to identify low-rank submatrices. Furthermore, the figure also demonstrates that the probability of hitting a near-rank-1  $2 \times 2$  submatrix is generally larger than in the case of Figure 7 since the planted near-rank-1 submatrices contain a large number of  $2 \times 2$  rank-1 submatrices. Finally, the figure confirms that SAMPLEANDEXPAND expands many initial submatrices into larger matrices with  $F_1$  score close to 1 and reconstruction error close to 0, suggesting that the ground-truth submatrix is recovered in many iterations.

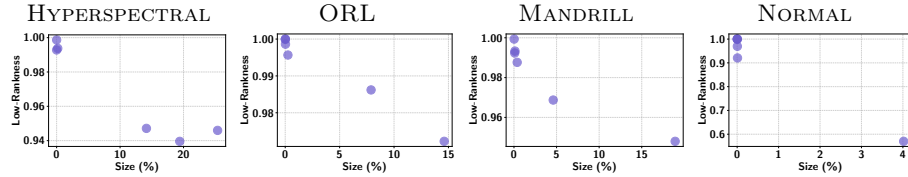


Fig. 9: Experiments on four example datasets (HYERSPECTRAL, ORL, GOOGLE and a  $250 \times 250$  synthetic dataset with i.i.d normally-distributed entries) to investigate the impact of  $\delta$  on the output of SAMPLEANDEXPAND. Each point indicates the low-rankness score and the percentage of entries of the discovered submatrices for a given value of  $\delta$ , with  $\delta \in \{10^{-6}, 10^{-5}, 10^{-4}, 10^{-3}, 10^{-2}, 10^{-1}\}$ .

**Experiments on synthetic and real-world data: impact of tolerance parameter.** The results provided by SAMPLEANDEXPAND vary with  $\delta$ . Intuitively, this parameter indirectly bounds the approximation error and thereby it embodies the trade-off between submatrix size and low-rankness. In more detail, a larger value of  $\delta$  leads to denser indicator matrices  $\mathbf{I}$  and thus larger output submatrices  $\mathbf{X}$ . On the other hand, a smaller value of  $\delta$  leads to generally smaller output submatrices  $\mathbf{X}$  which, however, may have higher low-rankness. In practice, SAMPLEANDEXPAND returns high-quality results across reasonable choices of  $\delta$ . In Figure 9 we show, for four examples example datasets (HYERSPECTRAL, ORL, MANDRILL and a synthetic  $250 \times 250$  matrix with i.i.d. entries drawn from a standard normal distribution and no planted near-rank-1 submatrices), the low-rankness score against the size of the submatrices output by SAMPLEANDEXPAND for different choices of the parameter  $\delta$ . Specifically, we vary  $\delta$  in  $\{10^{-5}, 10^{-4}, 10^{-3}, 10^{-2}, 10^{-1}\}$ . As for all the experiments in real-world datasets, the results in Figure 9 are obtained by relying on spectral biclustering for approximating maximum-edge bicliques. As a consequence, it is not guaranteed that larger values of  $\delta$  lead to larger size and lower low-rankness. Nevertheless, the results confirm that, also in the case where maximum-edge bicliques are approximated, larger values of  $\delta$  generally result in submatrices of larger size and lower low-rankness. Moreover, SAMPLEANDEXPAND outputs high-quality submatrices for any appropriate choice of  $\delta$ .

**Experiments on synthetic data: impact of noise.** To demonstrate the robustness of SAMPLEANDEXPAND to noise, Figure 10 shows results for the performance of different methods in near-rank-1 submatrix recovery as the level of noise increases. We use the same experimental setup as for the results shown in Figure 5, except that the dimension of the planted ground-truth near-rank-1 submatrix is held fixed to  $75 \times 75$  and the scale of the noise  $\epsilon_{\text{noise}}$  is varied in  $\{10^{-8}, 10^{-7}, 10^{-6}, 10^{-5}, 10^{-4}\}$ . The figure highlights that, in this setting, SAMPLEANDEXPAND and RPSP outperform the other baselines. Most importantly, the results resemble those shown in Figure 5 for planted submatrices of size  $75 \times 75$ , confirming that SAMPLEANDEXPAND is fairly robust to noise.

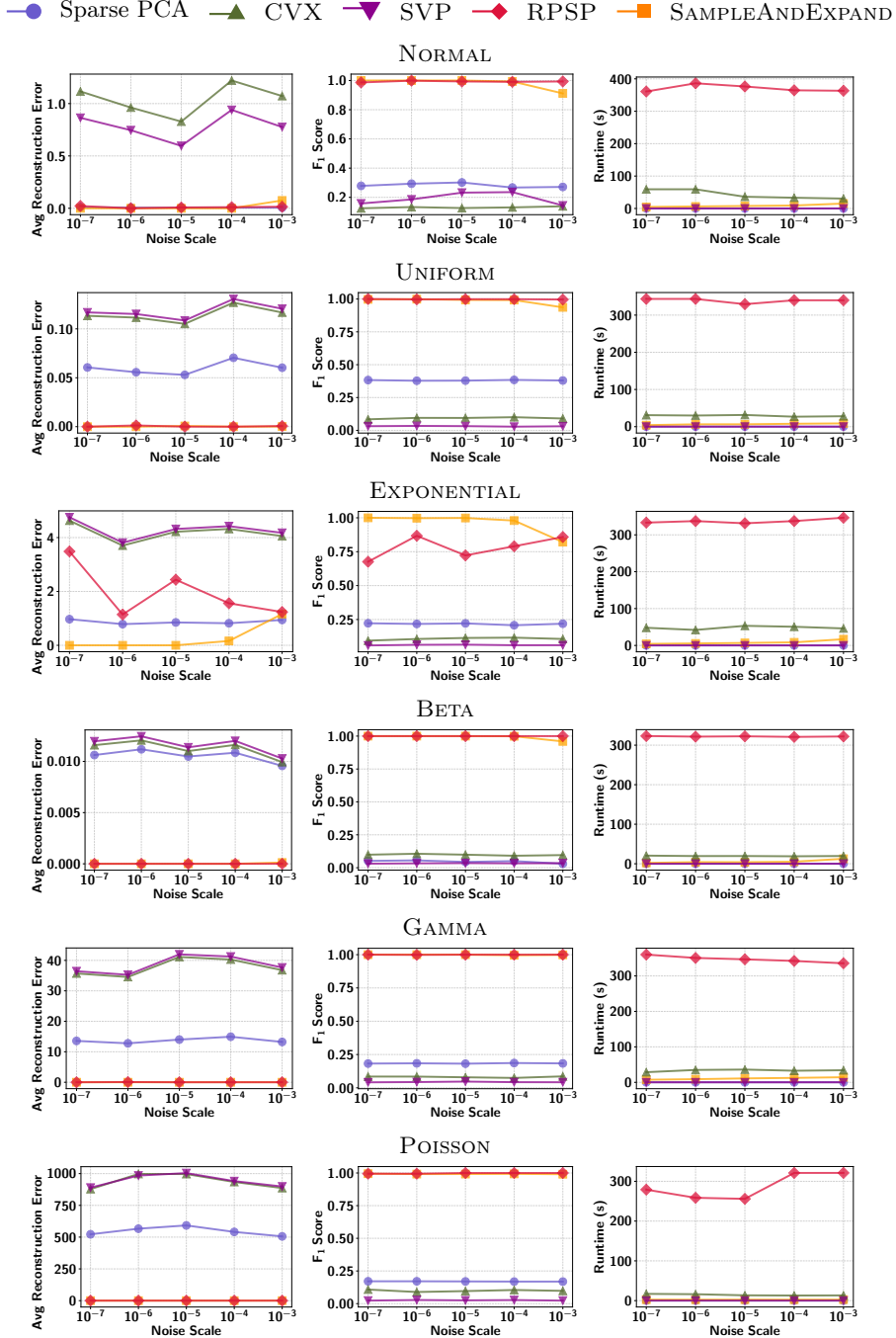


Fig. 10: Full-rank synthetic  $250 \times 250$ -matrices generated from different distributions with planted near-rank-1 submatrices of dimensions  $75 \times 75$ . Performance of different methods in the task of near-rank-1 submatrix discovery. We show the average (per-entry) reconstruction error (left), the  $F_1$  score (center) and the runtime (right) of the different methods under comparison as a function of the noise scale  $\epsilon_{\text{noise}}$ . The  $x$ -axis is on logarithmic scale.

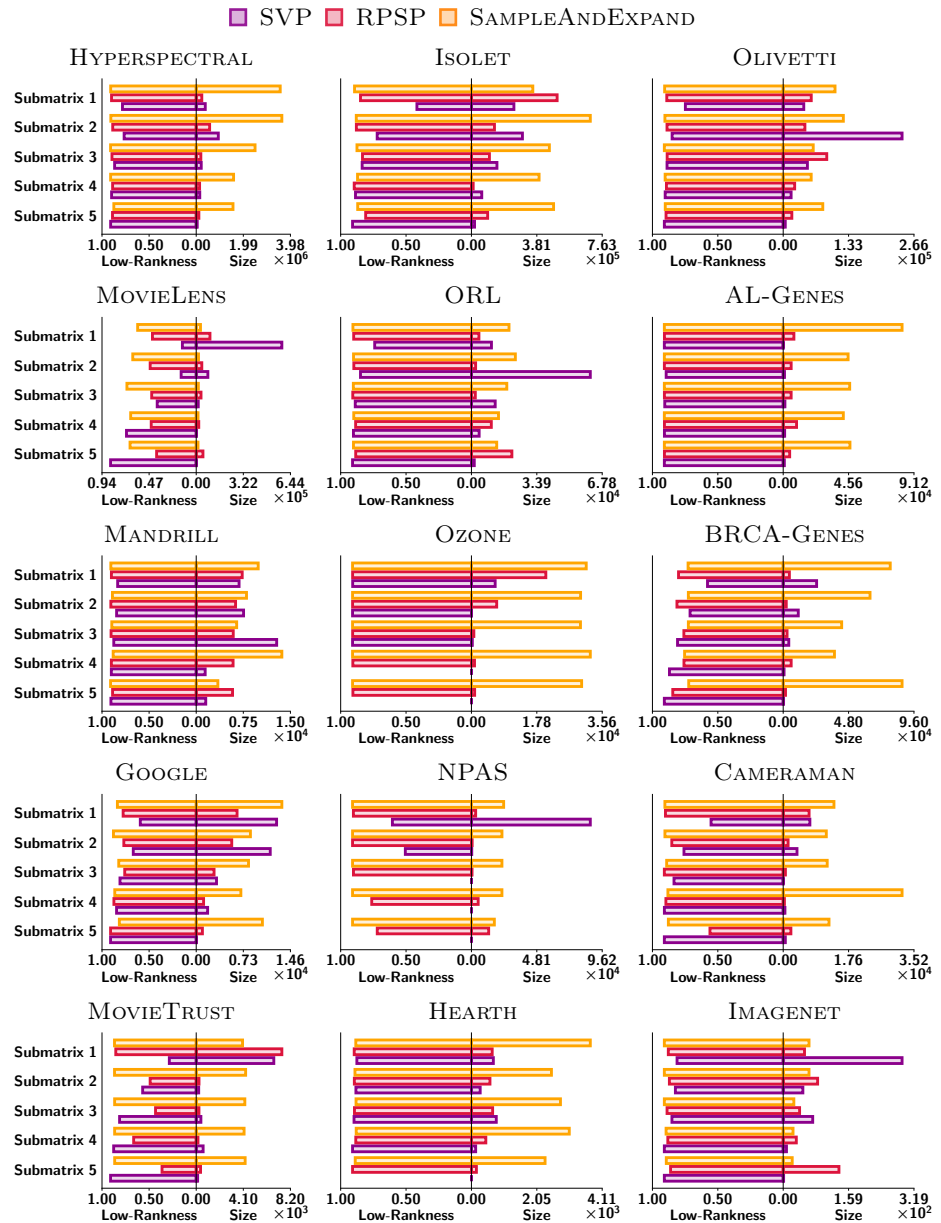


Fig. 11: Real-world datasets. Low-rankness score and size for each of the top-5 submatrices discovered by different methods.

**Experiments on real-world data: fine-grained results.** Table 2 shows average low-rankness and size of the top-5 low-rank submatrices retrieved by our method, RPSP and SVP for three datasets. In addition, Figure 11 provides a more fine-grained picture of the results of the experiments for all real-world datasets, showing the raw low-rankness score and the size (i.e., the number of entries) of each of the individual top-5 submatrices retrieved by SVP, RPSP and SAMPLEANDEXPAND. Note that, in three datasets (NPAS, OZONE and HEARTH), for SVP, results for less than 5 submatrices are shown because SVP is not able to discover five distinct submatrices.

## References

1. Agarwal, P.K., Procopiuc, C.M.: Approximation algorithms for projective clustering. *Journal of Algorithms* **46**(2), 115–139 (2003)
2. Asuncion, A., Newman, D., et al.: Uci machine learning repository (2007)
3. Boley, M., Lucchese, C., Paurat, D., Gärtner, T.: Direct local pattern sampling by efficient two-step random procedures. In: ACM SIGKDD. pp. 582–590 (2011)
4. Boutsidis, C., Mahoney, M.W., Drineas, P.: An improved approximation algorithm for the column subset selection problem. In: SODA. pp. 968–977 (2009)
5. Cambridge, A.L.: The orl database of faces (1994), <https://cam-orl.co.uk/facedatabase.html>
6. Ciaperoni, M., Gionis, A., Mannila, H.: The Hadamard decomposition problem. *Data Mining and Knowledge Discovery* pp. 1–42 (2024)
7. Dang, P., et al.: Generalized matrix local low rank representation by random projection and submatrix propagation. In: ACM SIGKDD. pp. 390–401 (2023)
8. Deng, J., Dong, W., Socher, R., Li, L.J., Li, K., Fei-Fei, L.: Imagenet: A large-scale hierarchical image database. In: 2009 IEEE conference on computer vision and pattern recognition. pp. 248–255. Ieee (2009)
9. Dhillon, I.S.: Co-clustering documents and words using bipartite spectral graph partitioning. In: ACM SIGKDD. pp. 269–274 (2001)
10. Doan, X.V., Vavasis, S.: Finding approximately rank-one submatrices with the nuclear norm and  $l_1$ -norm. *SIAM Journal on Optimization* **23**(4), 2502–2540 (2013)
11. Esposito, F.: A review on initialization methods for nonnegative matrix factorization: Towards omics data experiments. *Mathematics* **9**(9), 1006 (2021)
12. Gillis, N., Glineur, F.: Using underapproximations for sparse nonnegative matrix factorization. *Pattern recognition* **43**(4), 1676–1687 (2010)
13. Gillis, N., Shitov, Y.: Low-rank matrix approximation in the infinity norm. *Linear Algebra and its Applications* **581**, 367–382 (2019)
14. Golub, G.H., Van Loan, C.F.: Matrix computations. JHU press (2013)
15. Guo, Q., Zhang, C., Zhang, Y., Liu, H.: An efficient SVD-based method for image denoising. *IEEE transactions on Circuits and Systems for Video Technology* **26**(5), 868–880 (2015)
16. Harper, F.M., Konstan, J.A.: The movielens datasets: History and context. *Acm transactions on interactive intelligent systems (tiis)* **5**(4), 1–19 (2015)
17. Hu, E.J., Shen, Y., Wallis, P., Allen-Zhu, Z., Li, Y., Wang, S., Wang, L., Chen, W., et al.: Lora: Low-rank adaptation of large language models. *ICLR* **1**(2), 3 (2022)
18. Kaggle: Kaggle: Your machine learning and data science community (2024), <https://www.kaggle.com>

19. Kluger, Y., Basri, R., Chang, J.T., Gerstein, M.: Spectral biclustering of microarray data: coclustering genes and conditions. *Genome research* **13**(4), 703–716 (2003)
20. Lee, J., Kim, S., Lebanon, G., Singer, Y., Bengio, S.: Llorma: Local low-rank matrix approximation. *Journal of Machine Learning Research* **17**(15), 1–24 (2016)
21. Leone, G., et al.: Hyperspectral reflectance dataset of pristine, weathered and biofouled plastics. *Earth System Science Data Discussions* **2022**, 1–24 (2022)
22. Lyu, B., Qin, L., Lin, X., Zhang, Y., Qian, Z., Zhou, J.: Maximum biclique search at billion scale. *Proceedings of the VLDB Endowment* (2020)
23. Mahoney, M.W., Drineas, P.: Cur matrix decompositions for improved data analysis. *Proceedings of the National Academy of Sciences* **106**(3), 697–702 (2009)
24. Mairal, J., Bach, F., Ponce, J., Sapiro, G.: Online dictionary learning for sparse coding. In: *ICML*. pp. 689–696 (2009)
25. Miettinen, P., Neumann, S.: Recent developments in boolean matrix factorization. In: *IJCAI* (2021)
26. Ruchansky, N., Crovella, M., Terzi, E.: Targeted matrix completion. In: *SIAM SDM*. pp. 255–263 (2017)
27. Saw, J.G., Yang, M.C., Mo, T.C.: Chebyshev inequality with estimated mean and variance. *The American Statistician* **38**(2), 130–132 (1984)
28. University of Southern California, S., Institute, I.P.: Usc-sipi image database (2024), <https://sipi.usc.edu/database/>
29. Strang, G.: *Introduction to linear algebra*. SIAM (2022)
30. Tomczak, K., Czerwińska, P., Wiznerowicz, M.: Review the cancer genome atlas (tcga): an immeasurable source of knowledge. *Contemporary Oncology/Współczesna Onkologia* **2015**(1), 68–77 (2015)
31. Vidal, R.: Subspace clustering. *IEEE Signal Processing* **28**(2), 52–68 (2011)
32. Wang, Y., Zhu, L.: Research and implementation of SVD in machine learning. In: *ICIS*. pp. 471–475 (2017)